Beyond self-healing: Stabilizing and destabilizing photochemical adjustment of the ozone layer

Aaron Match[1], Edwin P. Gerber[1], and Stephan Fueglistaler[2]

[1]Center for Atmosphere Ocean Science, Courant Institute of Mathematical Sciences, New York University, New York, NY, USA

[2]Program in Atmospheric and Oceanic Sciences, and Department of Geosciences, Princeton University, Princeton, NJ, USA

Correspondence: Aaron Match (aaron.match@nyu.edu)

Abstract. The ozone layer is often noted to exhibit *self-healing*, whereby ~~a process that depletes ozone can nonetheless lead to increased ozone at lower altitudes. Self-healing has been explained to occur because ozone depletion aloft allows more ultraviolet (UV) light to reach lower levels, where it enhances ozone production~~ depletion of ozone aloft induces ozone increases below, explained to result from enhanced ozone production due to the associated increase in UV radiation below. Similarly, ~~a process that increases ozone can nonetheless~~ ozone enhancement aloft can reduce ozone below ~~, known as~~ (reverse self-healing). This paper considers self-healing and reverse self-healing to manifest a ~~more~~ general mechanism we call *photochemical adjustment*, whereby ozone perturbations lead to a downward cascade of anomalies in ~~ultraviolet fluxes~~ UV and ozone. Conventional explanations for self-healing ~~suggest~~ imply that photochemical adjustment is stabilizing, ~~i.e., the initial perturbation in column ozone is damped~~ damping perturbations towards the surface. However, photochemical adjustment can be destabilizing if the enhanced ~~ultraviolet transmission due to ozone depletion~~ UV disproportionately increases the ozone sink, ~~then photochemical adjustment can be destabilizing. We use the coefficients of the Cariolle v2.9 linear ozone model to~~ as can occur if that UV photolyzes ozone to produce atomic oxygen that speeds up catalytic destruction of ozone. We analyze photochemical adjustment in ~~the chemistry-climate model MOBIDIC. We find~~ two linear ozone models (Cariolle v2.9 and LINOZ), finding that: (1) photochemical adjustment is destabilizing ~~in the upper~~ above 40 km in the tropical stratosphere, and (2) self-healing ~~is often just the tip of the iceberg of large photochemical stabilizationthroughout the mid- and lower-stratosphere. The photochemical regimes from MOBIDIC can be reproduced by the Chapman Cycle, a classical modelof ozone photochemistry whose simplicity admits theoretical insight. Photochemical regimes in~~ often represents only a small fraction of the total photochemical stabilization. The destabilizing regime above 40 km is reproduced in a much simpler model: the Chapman Cycle ~~are controlled by the spectral structure of the perturbed ultraviolet fluxes. The transition from photochemical destabilization to stabilization occurs at the slant column ozone threshold where ozone becomes optically saturated in the overlap window of~~ augmented with destruction of O and O_3 by generalized catalytic cycles and transport (the *Chapman+2 model*). The Chapman+2 model reveals that photochemical destabilization occurs where the ozone sink is more sensitive than the source to perturbations in overhead column ozone, which is found to occur if the window of overlapping absorption by O_2 and O_3 is optically unsaturated, i.e., where overhead slant column ozone is below approximately 10^{18} molec cm^{-2} ~~(around 40 km in the tropics)~~.

1 Introduction

~~Earth's atmosphere is shaped primarily by just three radiatively-active gases: water vapor, carbon dioxide, and ozone~~

The ozone layer and ultraviolet (UV) fluxes are tightly coupled. UV radiation photolyzes O_2 into atomic oxygen, which can then bond with O_2 to form O_3. UV is also strongly absorbed by the ozone that has been formed. This absorption protects life at the surface while also photolyzing the O_3, reversing the formation reaction and feeding back onto the structure of the ozone layer. Thus does the absorption of UV lead to the continual destruction and reformation of the ozone layer, in the process attenuating the incoming UV flux at certain wavelengths by more than 30 orders of magnitude. ~~Water vapor is concentrated near the surface due to temperature-dependent condensation (e.g., Sherwood, 1996; Pierrehumbert and Roca, 1998; Galewsky et al., 2005). Carbon dioxide is well-mixed and evolves slowly subject to surface sources and sinks. Ozone, the focus of this paper, maximizes in the stratosphere where it shields the surface from dangerous ultraviolet radiation. Ozone is formed by photolysis and destroyed by both photolysis and catalytic chemistry.~~

The ~~photochemical nature of the ozone layer can cause~~ coupling between UV and O_3 can lead to counterintuitive responses to perturbations. ~~It is well known that~~ As was perhaps first noted by Johnston (1972), emitting an ozone-depleting substance whose local chemical effects strictly reduce ozone can nonetheless cause ozone to increase ~~in certain locations (Johnston, 1972; Dütsch, 1979; WMO, 1985; Solomon et al., 1985; Fomichev et al., 2007; Meul et al., 2014)~~at certain locations (subsequent treatments include Dütsch, 1979; WMO, 1985; Solomon et al., 1985; Fomichev et al., 2007; Meul et al., 2014). This phenomenon is known as *self-healing*. ~~Self-healing has been explained to occur because the reductions in ozone aloft allow more ultraviolet photons to reach lower altitudes, where they can increase the source of ozone enough to lead to net increases of ozone. Figure~~ Fig. 1a provides a canonical example of self-healing in response to ozone-depleting substances. The self-healing effect is visible as increases in ~~ozone~~ O_3 in the tropical lower stratosphere ~~(and upper troposphere)~~and tropical tropopause layer. Similarly, perturbations that locally increase ~~ozone~~ O_3 can lead to decreases in ~~ozone~~ O_3 known as reverse self-healing (Groves et al., 1978; Haigh and Pyle, 1982; Jonsson et al., 2004; WMO, 2018). ~~Figure~~ Fig. 1b provides a canonical example of reverse self-healing in response to stratospheric cooling from the direct radiative effects of elevated CO_2~~. Stratospheric cooling generally increases ozone but leads to reductions in the tropical lower stratosphere.~~ , the cooling from which changes collisional reaction rates to generally increase O_3, which then leads to reductions in the tropical lower stratosphere (op. cit.).

~~Explanations for self-healing and reverse self-healing invoke the fact that photolysis rates depend on attenuation of ultraviolet fluxes by overhead column ozone. Yet, despite invoking fundamental photochemical principles, self-healing and reverse self-healing typically only arise as curious aspects of the ozone response to perturbations (Figure 1).~~ Self-healing ~~or reverse self-healing have not been studied as objects of direct interest, and they are not described by a quantitative theory. This paper seeks to better understand self-healing and reverse self-healing, and to do so, we seek to understand the full consequences of the mechanism proposed to drive them. The driving mechanism of self-healing and reverse self-healing in response to a column ozone perturbation is the downward cascade of perturbation photolysis rates and perturbation column ozone. We define the component of the ozone response to a perturbation that results from changes in photolysis rates due to changes in overhead ozone as *photochemical adjustment*. Self-healing and reverse self-healing refer only to the subset of photochemical adjustment~~

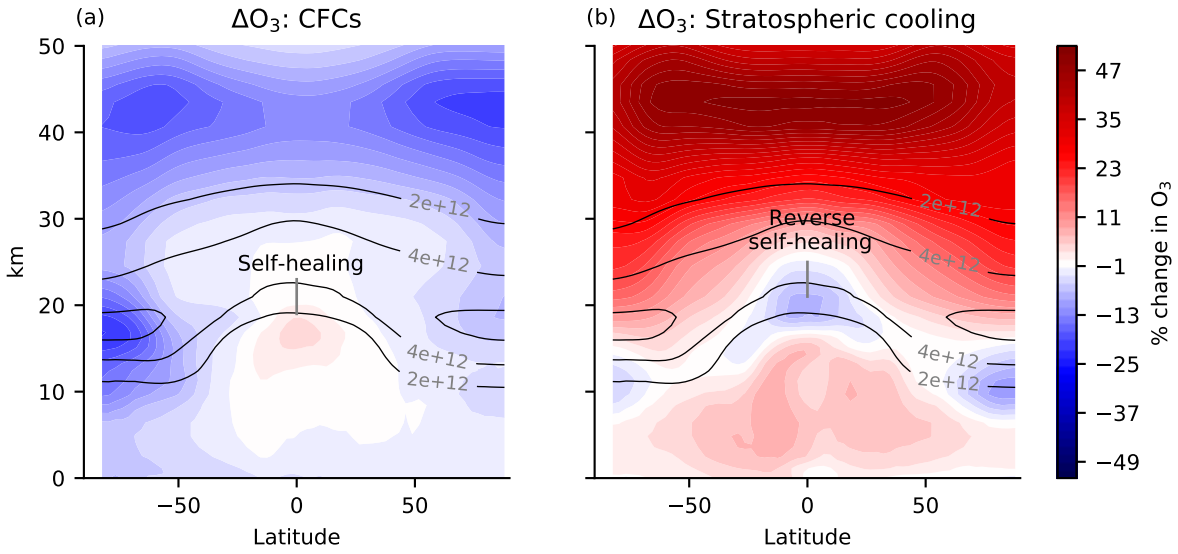

~~Canonical examples of self-healing and reverse self-healing. (a) Percent change in ozone in response to 2014 halocarbons (e.g., CFCs) imposed on a pre-industrial atmosphere (piClim-HC minus piControl) in MRI-ESM2-0, accessed from the CMIP6 archive. Halocarbons generally reduce ozone except in the tropical lower stratosphere, where there is self-healing. Pre-industrial control ozone is contoured in solid lines (molec cm^{-3}). (b) The ozone response to stratospheric cooling from a quadrupling of CO_2 with pre-industrial SST (piClim-4xCO2 minus piControl) in MRI-ESM2-0, accessed from the CMIP6 archive. Stratospheric cooling generally increases ozone except in the lower stratosphere where there is reverse self-healing.~~

Figure 1. Canonical examples of self-healing and reverse self-healing. (a) Percent change in ozone in response to 2014 halocarbons (e.g., CFCs) imposed on a pre-industrial atmosphere (piClim-HC minus piControl) in MRI-ESM2-0, accessed from the CMIP6 archive. The halocarbons generally reduce ozone, in particular also in the polar night vortex. However, in the tropical lower stratosphere ozone increases (self-healing). Pre-industrial control ozone is contoured in solid lines (molec cm^{-3}). (b) The ozone response to stratospheric cooling from a quadrupling of CO_2 with pre-industrial SST (piClim-4xCO2 minus piControl) in MRI-ESM2-0, accessed from the CMIP6 archive. Stratospheric cooling generally increases ozone except in the lower stratosphere where there is reverse self-healing. The increases in tropospheric ozone are due to processes not discussed here.

~~in which the sign of the ozone response to the perturbation is opposite what is expected, but photochemical adjustment is found to be a more general and fundamental mechanism of ozone photochemistry.~~

~~Photochemical adjustment is *stabilizing*, or compensating, if a reduction in column ozone overhead leads to an increase in ozone below. This increase in ozone will absorb ultraviolet radiation to counteract the effects of the initial reduction in column ozone, thereby damping the ultraviolet anomaly with altitude towards the surface. Self-healing and reverse self-healing both result from photochemical stabilization. Photochemical adjustment is *destabilizing*, or amplifying, if a reduction in column ozone overhead leads to a further reduction of ozone below, thereby amplifying photochemical anomalies towards the surface. Self-healing and reverse self-healing are typically explained in a way that would seem to preclude the possibility of~~

photochemical destabilization. This is because the net response of ozone is assumed to be determined by how the perturbation ultraviolet fluxes affect the ozone source. However, in ozone photochemistry, ultraviolet absorption can act as both a source *and* a sink of ozone. If the ozone sink were more sensitive than the ozone source to perturbations in overhead ozone, then reductions in ozone aloft that allowed more ultraviolet radiation to lower levels would lead to reductions in ozone below, i. e., photochemical destabilization.

Self-healing and reverse self-healing have historically been defined to occur where the sign of the ozone response is opposite that which is expected from the local perturbation. The more general phenomenon of photochemical adjustment cannot be defined merely by the sign of the ozone response, because photochemical stabilization can mute the ozone response to a perturbation without changing the sign of the net response, and photochemical destabilization amplifies the response without changing its sign. Thus, photochemical adjustment must be defined in terms of magnitudes. This paper develops a framework for defining and quantifying photochemical adjustment through the full ozone profile.

In Section **??**, we review current explanations for self-healing and reverse self-healing. Photochemical adjustment is defined, and we raise the possibility of photochemical destabilization. In Section 2, we quantify photochemical regimes in a chemistry-climate model with the aid of a pre-existing dataset: the coefficients of a linear ozone model. The atmosphere is found to exhibit both photochemical stabilization and photochemical destabilization. In Section 3, we propose a quantitative definition of photochemical adjustment. The coefficients of the linear ozone model are used to develop a photochemical adjustment emulator for a chemistry-climate model, which reveals that self-healing and reverse self-healing are just the tip of the iceberg of large photochemical adjustment throughout the entire ozone layer in response to perturbations. In Section 4, photochemical adjustment in the chemistry-climate model is shown to be strongly predictable from the Chapman Cycle of ozone photochemistry, despite its omission of key catalytic chemistry and transport. Possible reasons for this good fit are discussed. Based on the Chapman Cycle, a theory is developed in Section 5 for the transition altitude between photochemical destabilization and photochemical stabilization. Theoretical predictions of the transition altitude perform well in the chemistry-climate model. In Section 6, we develop a new qualitative explanation for photochemical adjustment that correctly extends to both photochemical stabilization and photochemical destabilization.

2 Qualitative explanations for self-healing and reverse self-healing

An early mention of "self-healing" was in a paper considering the ozone response to emissions of ozone-depleting substances from supersonic transports, when Johnston (1972) wrote, "These profiles include the partial self-healing effect of reformation of ozone at lower elevations." Self-healing or reverse self-healing have subsequently been been invoked in hundreds of papers when considering , covering the ozone layer response to CFCs (e.g., NAS, 1976), perturbations ranging from CFCs (e.g., NAS, 1976) and stratospheric cooling (e.g., Groves et al., 1978) , and the evolution of atmospheric oxygen to atmospheric oxidation (e.g., conceptually in Kasting and Donahue, 1980). Despite Yet despite being frequently invoked, self-healing and reverse self-healing have not been explained by a quantitative theory. They are seldom discussed in textbooks (although some qualitative descr Self-healing and reverse self-healing have mainly been invoked qualitatively and as are typically treated as curiosities only

needed to explain ~~unexpected~~ unexpectedly-signed responses of ozone to perturbations. ~~These invocations share a universal mechanism, yet some explanations also emphasize additional mechanisms.~~ They are only explained qualitatively, even in textbooks (e.g., Andrews et al., 1987; Finlayson-Pitts and Pitts, 2000).

~~The universal mechanism among explanations of self-healing is that when ozone is depleted~~ Self-healing is typically explained to result because ozone depletion aloft, such as from CFCs, ~~some~~ allows photons that would have been absorbed ~~by ozone aloft can~~ aloft to penetrate more deeply into the atmosphere~~. These photons can photolyze~~ , photolyzing O_2 ~~, a reaction that drives the production of ozone. If the enhanced production of ozone leads to a net increase of ozone compared to the unperturbed state, then this is called~~ down below to increase the source and concentration of O_3 (self-healing~~.~~). This mechanism relies on the spectral overlap between absorption by O_3 and O_2 at wavelengths less than 240 nm (e.g., Crutzen, 1974). The increased ozone from self-healing partially stabilizes the downwelling ultraviolet flux against the initial depletion of ozone. ~~When ozone is enhanced~~ Reverse self-healing is explained to result because ozone enhancement aloft, such as from stratospheric cooling, ~~the mechanism runs in reverse, leading to reverse self-healing: some~~ blocks photons that would have been absorbed by O_2 below~~are now intercepted by the enhanced~~ , reducing the source and concentration of O_3 ~~aloft. This reduces the ozone source below, and can lead to reductions of ozone, which again~~ below. Both self-healing and reverse self-healing partially stabilize the downwelling ultraviolet flux against the initial depletion of ozone~~. These two mechanisms for photochemical stabilization~~ , and are shown schematically in the top row of ~~Figure~~ Fig. 2.

~~As is noted in some studies, this universal explanation is premised on the substantial spectral overlap between absorption by O_3 and O_2 at wavelengths less than 240 nm. For example, Crutzen (1974) wrote: "This self-healing effect is due to deeper penetration~~

This standard explanation neglects the sensitivity of the ozone ~~producing ultraviolet radiation in the 2000-2300 Å200-230 nmregion." This overlap is necessary because self-healing results when absorption of photons switches from~~ sink to perturbations in UV fluxes. One reason that the ozone sink has been neglected is that photolysis of O_3 ~~at high altitudes to O_2 at low altitudes, and reverse self-healing results when absorption of photons switches from O_2 at low altitudes to O_3 at high altitudes.~~

~~Some explanations for self-healing and reverse self-healing invoke auxiliary mechanisms as well. We remark on two: first, some studies note that self-healing and reverse self-healing are muted by transport (Solomon et al., 1985)~~is typically considered to have a neutral effect on the ozone layer. This is because ~~self-healing and reverse self-healing tend to occur in the lower stratosphere, where photochemical equilibration times are slow enough that transport can induce substantial deviations in ozone from photochemical equilibrium. Second, some explanations note that the perturbation ultraviolet flux can drive photolysis reactions other than ozone production. When ozone is depleted aloft, the enhanced ultraviolet fluxes can also photolyze ozone, producing atomic oxygen . WMO (1985) noted that this atomic oxygen can then produce hydroxyl radicals that either produce ozone through smog chemistry or destroy ozone in catalytic cycles. Ozone production through the smog pathway leads to "ozone self-healing of the second kind". Although seldom discussed, this smog pathway might contribute to the increases of ozone in the upper troposphere in Figure 1a . Also seldom discussed but of central interest in this paper is that the perturbation atomic oxygen can also contribute to the destruction of ozone. If the perturbation ultraviolet fluxes can drive ozone destruction, then an underappreciated phenomenon becomes possible: self-amplified destruction.~~

Self-amplified destruction can occur if an photolysis of O_3 liberates an atomic oxygen that typically bonds with O_2 to reform O_3, completing a null cycle. Because the atomic oxygen is prone to reforming O_3perturbation aloft leads to perturbation UV fluxes that drive further net destruction of , it is standard to analyze ozone photochemistry in terms of odd oxygen ($O_x \equiv O + O_3$. This destruction of O_3 can result from the photolysis of), which is longer-lived than ozone and preserved by photolysis of O_3 , which produces O. Much of this Owill recombine with O_2 to reform O_3, completing a null cycle with no net effect on O_3, but some of the O can bond (e.g., Jacob, 1999; Brasseur and Solomon, 2005). However, this null cycle does not close perfectly, and leakage from the null cycle occurs if the atomic oxygen bonds with O_3 to destroy O_3, orcan bond (as in Chapman, 1930), or, as happens more often, with catalysts of O_3 depletion , indirectly destroying the Osuch as HO_2 or NO_2 (Bates and Nicolet, 1950; Crutzen, 1970). Although small compared to the null cycle, this leakage means that UV can drive a photolytic sink of $O_3$by virtue of not closing the null cycle. To the extent that there is leakage . In other words, although odd oxygen is preserved by photolysis of Ofrom the null cycle into other reactions that destroy O_3, photolysis of , the sink of odd oxygen is nonetheless sensitive to such photolysis.

The photolytic sink of O_3 becomes a sink of opens unconventional possibilities for the O_3 response to perturbations in overhead column O_3. Self-amplified destruction is photochemically destabilizing, meaning that the perturbation ultraviolet flux grows with altitude towards the surface. Running this response in reverse, a perturbation that added ozone aloft could reduce the ozone sink belowto lead to enhanced ozone belowIf at some altitude the photolytic sink of ozone is more sensitive than the photolytic source, then O_3 depletion aloft would lead to a net enhancement of the O_3 sink below, further depleting O_3 below (*self-amplified destruction*). Likewise, O_3 addition aloft would lead to a net reduction in the O_3 sink below, further adding O_3 below (*self-amplified production*). Figure 2 Both of these responses are photochemically destabilizing, causing photochemical perturbations to amplify towards the surface. Fig. 2 (bottom row) illustrates these two eases mechanisms of photochemical destabilization.

Photochemical stabilization is typically explained with the mechanisms in the top row. (Top left) Depletion of ozone aloft allows deeper penetration of UV that can increase the ozone source and produce additional ozone, potentially leading to self-healing. (Top right) Addition of ozone aloft prevents deeper penetration of UV, decreasing the ozone source below and removing ozone, potentially leading to reverse self-healing. Photochemical destabilization is proposed to result from the mechanisms in the bottom row. (Bottom left) Depletion of ozone aloft allows deeper penetration of UV that can increase the ozone sink leading to self-amplified destruction. (Bottom right) Addition of ozone aloft prevents deeper penetration of UV, decreasing the ozone sink below and increasing ozone, leading to self-amplified production.

Conventional explanations for self-healing and reverse self-healing do not hint at the possibility of photochemical destabilization . Instead, these explanations imply that the net change in ozone is dictated by the changes in the photolytic source alone, without considering possible changes in the photolytic sink. Yet, the prospect of photochemical destabilization can be traced back to Photochemical destabilization has been noted before, in Hartmann (1978), who identified significant photochemical destabilization above 40 km in a simple modelof the ozone layer. The prospect of photochemical destabilization has been neglected in the intervening decades modified Chapman Cycle model. However, they disclaimed their results as unrealistic, and it has since been neglected, perhaps for two main reasons. The first reason is theoretical: photolysis of ozone has been treated as having

no net effect on ozone because of the significant null cycle, whereas photochemical destabilization requires that photolysis of ozone destroys some amount of ozone. The second reason is practical: : (1) it was considered theoretically impossible due to conceptual neglect of the photolytic sink of O_3, and (2) it was hiding, because self-healing and reverse self-healing demand an explanation because the sign of the ozone response is unexpectedby virtue of their unexpected sign compared to that of the initial perturbation, whereas photochemical destabilization demands no such explanation because it does not change the sign of the ozone response . Photochemical destabilization can only be distinguished by the *magnitude* of the response, and thus, in the absence of quantitative treatments, photochemical destabilization would be aliased into the local response of the ozone layer to the initial perturbation . De-aliasing photochemical destabilization begins by quantifying the sensitivity of ozone photochemistry to perturbations in column ozone, as calculated in a chemistry-climate model in the next section. to a perturbation.

We find that photochemical destabilization is not only theoretically possible, but is actually revealed in the coefficients of two linear ozone models (Cariolle v2.9 and LINOZ) in the tropical stratosphere above 40 km, exactly where it was first noted in Hartmann (1978) (Section 2). To better characterize these sensitivities, we generalize photochemical stabilization and destabilization as manifesting the broader phenomenon of *photochemical adjustment*, defined as the component of the O_3 response to a perturbation that is mediated by changes in UV from overhead column O_3 responses to that same perturbation (Section 3). Photochemical adjustment is quantified by the difference between the response to a perturbation under interactive versus locked UV. The region of photochemical destabilization above 40 km is then reproduced in a highly simplified model of the Chapman Cycle augmented with two generalized sinks of O and O_3 to represent catalytic cycles and transport—the *Chapman+2 model* (Section 4). The Chapman+2 model facilitates the development of a theory for the transition altitude between photochemical destabilization and photochemical stabilization (Section 5). This theory reproduces the latitudinal structure of the region of photochemical destabilization. In Section 6, we develop a new qualitative explanation for photochemical adjustment that is consistent with these quantitative insights.

2 Photochemical regimes in ~~a chemistry-climate model~~linear ozone models

An ideal test of To assess whether the ozone layer is photochemically stabilizing or destabilizing in at a given locationis to calculate , we evaluate the sensitivity of the local net production rate of ozone to an ultraviolet (production minus loss) to a UV perturbation induced by some change in the overlying column ozonea change in overhead column O_3, holding all else fixed (including tendencies from transport). Increasing the overlying column ozone will decrease the incoming photons overhead column O_3 decreases the photons reaching a given altitude in accord with the spectrally-varying absorption of ozone and the magnitude of the perturbation. This perturbation to the incoming photons can modify both ozone production and destruction, so the key response variable is the change in , reducing the photolysis rates of both O_2 and O_3 that drive the net production rateof ozone (i. e., production minus loss). If an increase in the overlying column ozone . If the increase in overhead column O_3 reduces the net production rate, then that location is in a photochemically stabilizing regime. If an increase in the overlying column ozone that leads to photochemical stabilization. If the increase in overhead column O_3 increases the net production

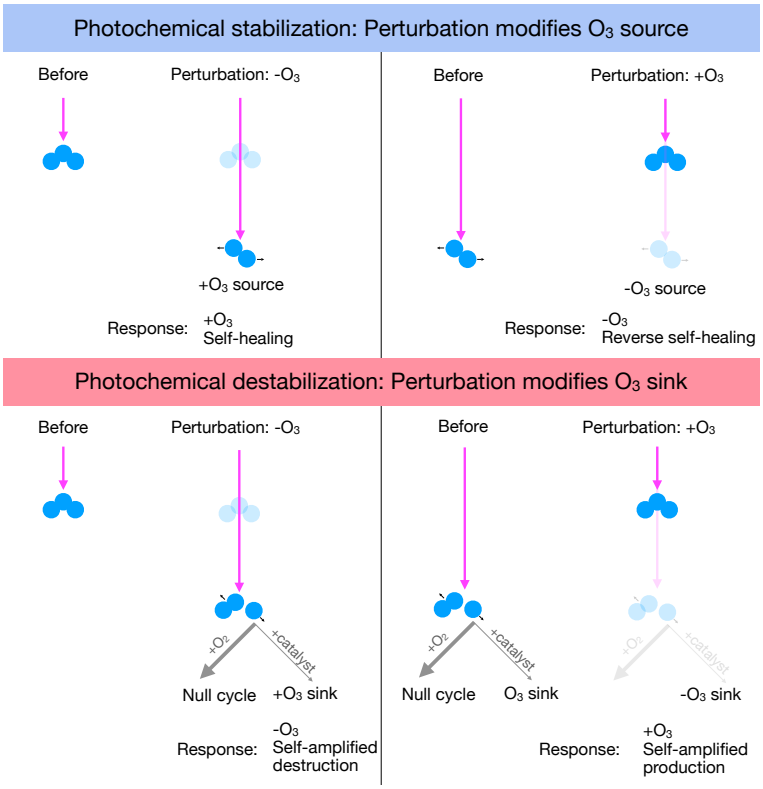

Figure 2. (Top row) Photochemical stabilization is typically explained as follows: (top left) Depleting O_3 aloft allows deeper penetration of UV that photolyzes O_2 to increase the O_3 source and add O_3, causing self-healing; (top right) Adding O_3 aloft blocks deeper penetration of UV, decreasing the photolysis of O_2 to decrease the O_3 source below and depleting O_3, causing reverse self-healing. (Bottom row) Photochemical destabilization is proposed as follows: (bottom left) Depleting O_3 aloft allows deeper penetration of UV that can increase photolysis of O_3, primarily driving a null cycle but with leakage that speeds up catalytic destruction of O, enhancing the ozone sink and further depleting ozone (self-amplified destruction); (bottom right) Adding ozone aloft blocks deeper penetration of UV that would have driven this catalytic destruction of O, the reduction in which reduces the O_3 sink below and adds further O_3 (self-amplified production).

rate, ~~then that location is in a photochemically destabilizing regime~~that leads to photochemical destabilization. To characterize a climatology of photochemical regimes, this test ~~would have to~~ must be repeated at all latitudes, altitudes, and seasons.

This exact battery of ~~regime~~ tests has been performed in ~~chemistry-climate~~ chemical transport models by previous studies that developed linear ozone models, two independent sets of coefficients from which are used throughout this study: Cariolle v2.9 (Cariolle and Déqué, 1986; Cariolle and Teyssèdre, 2007) and LINOZ (McLinden et al., 2000). Linear ozone models are tools for computationally speeding up chemistry-climate modeling of ozone. In a linear ozone model, the net tendencies of ozone from a ~~chemistry-climate~~ chemical transport model with 10s-100s of (photo-)chemical reactions are linearized with respect to finite perturbations in local ozone concentration, temperature, and overhead column ozone. Then, for computational

efficiency, the ozone module can be replaced with these linear functions evaluated using their table of coefficients. A standard linear ozone model equation, first proposed in Cariolle and Déqué (1986), is as follows:

$$\frac{dr_{O_3}}{dt} = A_1 + A_2(r_{O_3} - A_3) + A_4(T - A_5) + A_6(\chi_{O_3} - A_7) \quad (1)$$

where r_{O_3} is the ozone mixing ratio, $A_1 = P - L$ is the basic state photochemical production minus loss rate, $A_2 = \partial(P - L)/\partial r_{O_3}$, A_3 is the basic state ozone mixing ratio, $A_4 = \partial(P-L)/\partial T$, A_5 is the basic state temperature, $A_6 = \partial(P-L)/\partial\chi_{O_3}$ where χ_{O_3} is the ~~overlying~~ overhead column ozone $\int_z^\infty [O_3]dz$ in units of [molec cm^{-2}] and [O_3] is the ozone number density [molec cm^{-3}], and A_7 is the basic state overhead column ozone.

~~We propose to interpret the~~ The linear ozone model coefficients are interpreted as classifying the photochemical regime based on the sign of the sensitivity to perturbations in column ozone (A_6). Photochemical stabilization occurs where $A_6 < 0$, meaning that an increase in overhead ozone reduces the net ozone production. Photochemical destabilization occurs where $A_6 > 0$, meaning that an increase in overhead ozone increases the net ozone production.

Previous studies have calculated the A parameters within ~~a chemistry-climate model~~ chemical transport models as functions of altitude, latitude, and month. We have globally analyzed the A_6 coefficients in ~~the Cariolle v2.9 linear ozone model. We thank Daniel Cariolle for sharing the~~ two models. The first (and primary) linear ozone model ~~with us. The~~ we evaluate is the Cariolle v2.9 linear ozone model ~~is descended from the first linear ozone model, with a major update to include heterogeneous chemistry (not directly relevant to this work)in Cariolle and Teyssèdre (2007)~~(coefficients obtained by personal communication with Daniel Cariolle). The Cariolle linear ozone model is ~~based on the chemistry-climate~~ linearized with respect to the chemical transport model MOBIDIC, first described in Cariolle and Brard (1984). ~~The transport is~~ MOBIDIC is driven by 2D transport based on the residual circulation. The first linear ozone model was described in Cariolle and Déqué (1986), from which the Cariolle v2.9 linear ozone model descended, with a major update to specify the 2D circulation from the ARPEGE-Climat model (Déqué et al., 1994) and to include heterogeneous chemistry in Cariolle and Teyssèdre (2007). The recent version of MOBIDIC to which the Cariolle v2.9 linear ozone model is calibrated includes the main gas-phase reactions driving the NOx, HOx, ClOx, and BrOx catalytic cycles, with 30 transported long-lived species and 30 short-lived species computed diagnostically (Cariolle and Teyssèdre, 2007). The Cariolle linear ozone model has been shown to perform well compared to state-of-the-art comprehensive chemistry-climate models (Meraner et al., 2020) and is used to prognose ozone in the ERA5 reanalysis (Hersbach et al., 2020). The second linear ozone model we evaluate is the LINOZ scheme, based on the UC Irvine chemical transport model (e.g., as used in Hall and Prather, 1995) driven by the general circulation from NASA GISS ModelE (coefficients obtained by personal communication with Clara Orbe). LINOZ is documented in McLinden et al. (2000), and recent implementations include Rind et al. (2014) and DallaSanta et al. (2021).

The values of A_6 during the month of March (chosen as an equinoctial month) are shown ~~in Figure 3a~~for Cariolle v2.9 and LINOZ in Figs. 3a,b. Negative values indicate photochemical stabilization, and positive values indicate photochemical destabilization. A major result is that there is significant and large photochemical destabilization, primarily above 40 km. This

means that ozone depletion above 40 km removes additional ozone down to 40 km. Because these two linear ozone models agree so strongly, further analyses will focus on the Cariolle v2.9 model unless otherwise noted.

Photochemical destabilization occurs ~~above the maximum number densities of O_3~~well above the bulk of the ozone layer; as evaluated using the climatological structure of O_3 in ~~MOBIDIC~~the Cariolle v2.9 coefficients, 4% of ozone molecules in the deep tropics (from 20°S-20°N) are in a photochemically destabilizing regime above 40 km. Despite including only a modest fraction of O_3, this region of photochemical destabilization challenges prevailing theory, which only emphasizes the photochemical sensitivity of the ozone source and therefore cannot account for destabilization.

Intriguingly, the photochemical destabilization above 40 km in the tropics is located where it was first noted in Hartmann (1978) ~~for the~~ in their modified Chapman Cycle model. ~~The Chapman Cycle model only involves four chemical reactions—two photolysis reactions and two combination reactions—yet has been shown to capture many gross features of the ozone layer, such as the overall shape of the ozone layer (Chapman, 1930; Jacob, 1999). Figure 3b shows~~ We reproduce the transition from destabilization aloft to stabilization below in our own version of the Chapman Cycle augmented with generalized sinks of O and O_3 from transport and catalytic cycles. These sinks are represented as two generalized chemical reactions, hence our model is called the *Chapman+2 model*. The photochemical sensitivity of the ~~net ozone production rate for a Chapmanphotochemical equilibrium to perturbations in column ozone. This Chapman Cycle result has been placed beside the Cariolle v2.9 result to emphasize that the Chapman Cycle reproduces the map of the photochemical regimes.~~ Chapman+2 model is shown in Fig. 3c, which reproduces key features from the linear ozone models, which are in turn based on much more complex photochemical models. The details of the Chapman~~Cycle result and the theory (magenta curves)~~ +2 model results will be presented later in Section 4.

The coefficients of the Cariolle v2.9 linear ozone model have provided exactly the evidence needed to classify regions of the atmosphere as photochemically stabilizing or destabilizing. One striking feature of ~~Figure 3a~~Figs. 3a,b is that the sensitivity of the net ozone production rate to perturbations in column ozone has a larger magnitude in the destabilizing region than in the stabilizing region. This might seem to imply that destabilization is stronger than stabilization. However, the basic state production and loss are also larger in the upper atmosphere, where the ~~actinic~~ UV flux has not been attenuated as strongly, so therefore the ozone equilibration timescale may also be relevant to considering the magnitude of photochemical stabilization. Questions about the magnitude of photochemical stabilization demand a method for quantifying the full vertical profile of photochemical adjustment in general, ~~a method we develop~~ developed in the following section.

3 Defining photochemical adjustment and quantifying it ~~in the~~ using a linear ozone model

~~Photochemical adjustment is~~ The idea behind photochemical stabilization or destabilization is that changes in ozone aloft can lead to a downward cascade of perturbations in ozone, yet this idea has not been previously formalized in a quantitative way. Here, we define *photochemical adjustment* as the component of the ozone response to a perturbation that results from changes in photolysis due to changes in column ozone aloft. ~~This is the idea behind self-healing—the surprising increase in ozone in the lower tropical stratosphere in simulations of ozone depletion is attributed to the increase in photons penetrating to lower~~

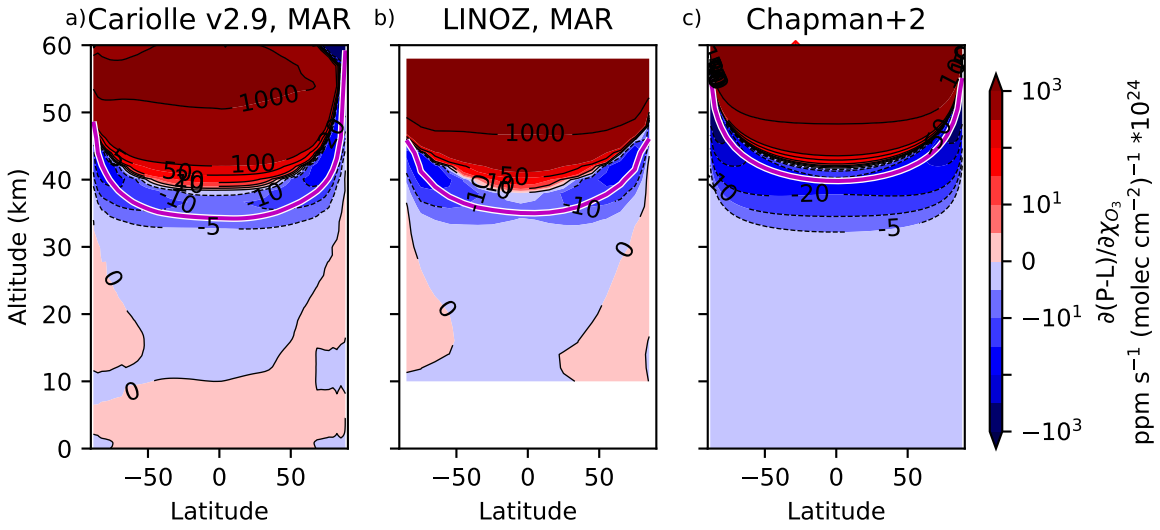

Figure 3. Sensitivity of net ~~ozone~~ odd oxygen photochemical production rate to perturbations in column ozone~~in (a) Cariolle v2.9 in~~ , calculated for the month of March (approximately equinoctial conditions such that latitude $\theta \approx$ solar zenith angle) in two linear ozone models: (a) Cariolle v2.9 based on MOBIDIC (Cariolle and Déqué, 1986) and (b) LINOZ based on UC Irvine CTM driven by NASA GISS ModelE (McLinden et al., 2000). The linear ozone model coefficients are compared to the Chapman+2 model, in which latitudinal dependence is represented by performing single-column calculations. Photochemical stabilization is indicated by negative values, whereas photochemical destabilization is indicated by positive values. Spectrally-resolved photochemical theory (Section 5) predicts positive coefficients where the slant ozone column is less than 10^{18} molec cm^{-2} (i.e., above the magenta curve).

~~levels—but to date it lacks a quantitative assessment. We therefore formally define the photochemical adjustment to an ozone perturbation~~ Photochemical adjustment is therefore quantified as the difference between a fully interactive simulation of ozone photochemistry~~and~~ , in which ozone and UV are coupled in the column through the photolysis rates, compared to one where the ~~UV-flux~~ UV fluxes (and hence ~~photons available for photolysis of O_2 and O_3) is held fixed~~photolysis rates) are locked at their unperturbed values:

$$\text{Photochemical adjustment} \equiv [\mathrm{O_3}]|_{\text{Fully Interactive}} - [\mathrm{O_3}]|_{\text{UV-Locked}} \tag{2}$$

This UV-locking method can in principle be implemented in any modeling context for atmospheric chemistry. Intuitively, a UV-locked simulation can be obtained in a ~~chemistry-climate model by fixing the overlying column ozone seen~~ photochemical model by locking the overhead column ozone when calculating photolysis rates~~at its unperturbed value~~, where the locked ozone could be steady or climatologically-evolving depending on the context. This ensures that the photolysis rates do not respond to any changes in ozone resulting from the perturbation, but allows all other ~~adjustments to the chemistry~~photochemical responses.

In this paper, we ~~will~~ implement this approach using two methods. First, we use the Cariolle v2.9 linear ozone model coefficients to develop a linear emulator ~~for analyzing ozone perturbations in MOBIDIC~~of photochemical adjustment. Later, we will perform various UV-locking experiments in the Chapman~~Cycle~~+2 model, which will be shown to reproduce essential ~~aspects of the chemistry-climate model.~~ results from the linear ozone model. Both of these analyses consider the equilibrated response to steady perturbations.

We begin our derivation for the linear emulator of the perturbation ozone equation by converting ozone anomalies in the linear ozone model from mixing ratio (~~Equation~~ Eq. 1) into number density (for convenience) by multiplying by the number density of air, denoted n_a [molec cm^{-3}]. We then decompose the variables in our prognostic ozone number density equation into basic state and perturbation components, $x = \bar{x} + x'$, where $\bar{x}$ is the basic state component and x' the perturbation. Subtracting the basic state component from the total equation ~~,~~and assuming a quasi-steady state~~allows us to~~ , we solve for the perturbation ozone number density ~~,~~as a function ~~height,~~ of height in the presence of some prescribed perturbation, G:

$$[\mathrm{O_3}]' = -\frac{A_4 n_a T'}{A_2} - \frac{A_6 n_a \chi'_{\mathrm{O_3}}}{A_2} + G \tag{3}$$

On the right-hand-side, the first term captures the sensitivity to temperature perturbations, the second term captures the sensitivity to overhead column ozone perturbations, thereby ~~encoding~~ coupling in the photochemical adjustment, and the third term is the prescribed perturbation in ozone. A_2 (defined as $\partial(P-L)/\partial r_{\mathrm{O_3}}$) tends to be negative, reflecting that local perturbations in ozone tend to decay on a timescale of $-1/A_2$. ~~While Equation~~ Although Eq. 3 is linear at any given height, it is mathematically implicit because the perturbation overhead column ozone is the integral of the ozone number density perturbation (i.e., $\chi'_{\mathrm{O_3}} = \int_z^\infty [\mathrm{O_3}]' dz$). Photochemical adjustment at height thus influences lower levels, introducing a spatial nonlinearity encoded in the A_6 term, and ~~one must solve the system downward~~ Eq. 3 must be solved from the top of the atmosphere downwards.

We ~~use the linear ozone model to quantify the response of the tropical ozone layer to~~ assess the response of tropical ozone ~~depletion and to stratospheric cooling .~~ to highly-idealized forcing by ozone depletion (e.g., from ozone depleting substances) and stratospheric cooling (e.g., from the direct radiative effects of CO_2). The response to such perturbations is generally known to have nontrivial vertical structure (e.g., Fig. 1), although this response already includes the effects of photochemical adjustment, whose structure we seek to isolate. In order to illustrate how photochemical adjustment can induce nontrivial vertical structure even in response to uniform perturbations, we consider constant (or piecewise-constant) perturbations. Ozone depletion is represented as a uniform reduction of ozone below its basic state value ($G = -G_0, T' = 0$), which in turn can induce photochemical perturbations by perturbing the ~~actinic~~ UV flux that drives ozone at lower levels. Thus, the fully interactive linear response to this uniform perturbation in ozone includes the perturbation itself plus the nonlocal effects of perturbed ~~actinic~~ UV flux. Stratospheric cooling is represented as a uniform cooling (G = 0, $T' = -\Delta T$), which tends to locally increase ozone. ~~These~~ This cooling is imposed uniformly, even extending into the troposphere, where the response is small but should not be considered as a realistic response to elevated CO_2, which instead (as is well known) warms the troposphere. The local increases in ozone ~~can~~ from these perturbations then perturb the ~~actinic flux~~UV fluxes, leading to a fully interactive response

that includes the local effects of cooling and the nonlocal effects of ~~column ozone changes aloft~~changes in overhead column ozone.

These two perturbations are explored by using the coefficients of the linear ozone model to perform an offline calculation of the linear response of a steady state ozone layer to ozone depletion or stratospheric cooling. The linear ozone model distills the relative importance of the local effects of ~~our~~ these perturbations from the non-local effects of the ~~actinic~~ UV flux perturbations from aloft, as conveyed by the sensitivity to overhead column ozone. Both of these offline calculations have been performed on the discrete grid of the Cariolle v2.9 linear ozone model, with levels z_i, i = 1-N numbered from the top of the atmosphere downwards, each with a ~~depth~~ thickness of Δz_i. Uniform ozone depletion with a magnitude G_0 has been imposed at and below $z_5 = 60$ km. The fully interactive ozone response to this perturbation has been calculated by iterating between calculating the ozone response at level i and the resulting overhead column ozone anomaly at level i that is then seen by level $i+1$. The initial anomaly is therefore $[\mathrm{O_3}]'(z_5) = -G_0$, which leads to ~~a~~ an overhead column ozone anomaly of $\chi'_{\mathrm{O_3}}(z_5) = -G_0 \Delta z_5$. The fully interactive response at z_6 can then be calculated as $[\mathrm{O_3}]'(z_6) = -G_0 - A_6 n_a \chi'_{\mathrm{O_3}}(z_5)/A_2$. This ozone anomaly is used to update the overhead column ozone perturbation as $\chi'_{\mathrm{O_3}}(z_6) = \chi'_{\mathrm{O_3}}(z_5) + [\mathrm{O_3}]'(z_6)\Delta z_6$. The solution can then proceed iteratively, where at each lower altitude, we first calculate the ozone perturbation, then add that ozone perturbation (multiplied by the layer ~~depth~~thickness) to the overhead column ozone perturbation.

A similar iterative method is used to calculate the response to stratospheric ~~cooling. Here, we consider a uniform cooling of ΔT throughout the atmosphere, a notable simplification on the actual stratospheric cooling in response to greenhouse gases given that we impose such cooling throughout the stratosphere and troposphere and with no vertical structure.~~ (and tropospheric) cooling. Our iterative calculation begins at the top of the ~~atmosphere~~ model (z_1 = 80 km) with a local ozone anomaly of $[\mathrm{O_3}]'(z_1) = A_4 n_a \Delta T/A_2$. This local ozone anomaly leads to ~~a~~ an overhead column ozone perturbation of $\chi'_{\mathrm{O_3}}(z_1) = [\mathrm{O_3}]'(z_1)\Delta z_1$. The ozone perturbation at the next lower altitude can then be calculated in general as $[\mathrm{O_3}]'(z_i) = A_4 n_a \Delta T/A_2 - A_6 n_a \chi'_{\mathrm{O_3}}(z_{i-1})/A_2$. The overhead column ozone perturbation can then be updated in general as $\chi'_{\mathrm{O_3}}(z_i) = \chi'_{\mathrm{O_3}}(z_{i-1}) + [\mathrm{O_3}]'(z_i)\Delta z_i$.

Using this approach, we calculated the linear response of ozone to uniform ozone depletion and stratospheric cooling. The response to these perturbations in the absence of photochemical adjustment can also be calculated directly as the UV-locked response by repeating the calculation with $\chi'_{\mathrm{O_3}}$ overwritten to zero everywhere. For uniform ozone depletion, the UV-locked response is simply the prescribed ozone depletion, a reduction by G_0 at all altitudes below 60 km. For stratospheric cooling, the UV-locked response is the direct thermal response given by the first term on the right-hand-side of ~~Equation~~ Eq. 3. Knowing the ~~photolysis-locked~~ UV-locked responses, it is then straightforward to calculate the photochemical adjustment~~using Equation 2as~~, which (per Eq. 2) is the Fully Interactive response minus the UV-Locked response.

The results are shown in ~~Figure~~ Fig. 4, as calculated using the linear ozone model coefficients in March for an equatorial atmospheric column. The response to uniform ozone depletion below 60 km of $G_0 = 10^8$ molec cm^{-3} is shown in ~~Figure~~ Fig. 4a, with the prescribed depletion shown in blue. The fully interactive response (black) differs substantially from the prescribed perturbation. The fully interactive response shows reductions of ozone in the upper stratosphere that are larger in magnitude than those prescribed, peaking at 42 km with an amplitude 75% larger than what is prescribed. This is a consequence of self-

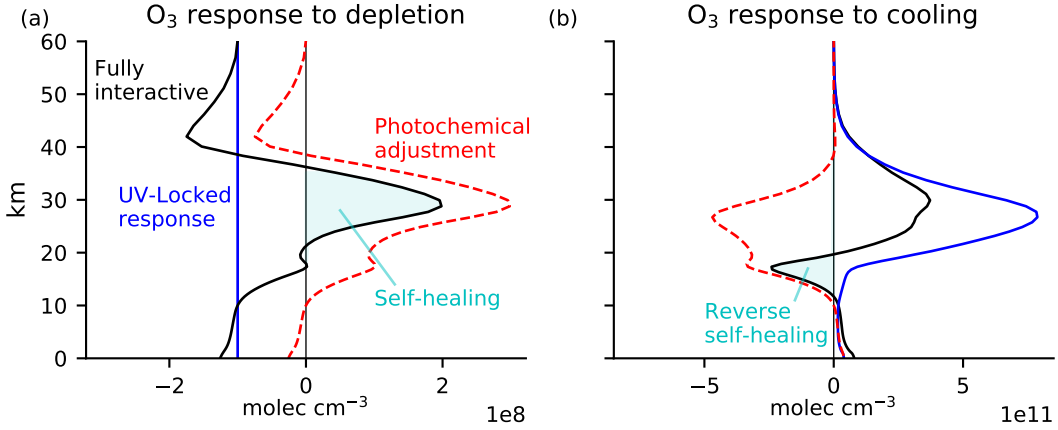

Figure 4. Ozone response to (a) uniform depletion by 10^8 molec cm^{-3} everywhere below 60 km and (b) uniform cooling of 10 K. The calculation is performed ~~in a linear emulator of MOBIDIC~~ by iteratively solving ~~Equation~~ Eq. 3 using coefficients from the Cariolle v2.9 linear ozone model. The Fully Interactive response (black) is decomposed into a UV-Locked response (blue) and photochemical adjustment (red). Self-healing and reverse self-healing (cyan shading) are merely the tip of the iceberg of large photochemical adjustment throughout the column, with photochemical destabilization above 40 km and photochemical stabilization below 40 km.

amplified destruction in the region of photochemical destabilization above 40 km. Below 40 km, the response is no longer photochemically destabilizing, and the fully interactive response is more positive than the prescribed reduction. At 35 km, the fully interactive response becomes positive in absolute ~~terms; this is self-healing, an increase in ozone driven by a perturbation that reduces ozone locally. The fully interactive~~ terms—self-healing. The absolute increase in ozone peaks at a value around $2G_0$ at 29 km; the associated photochemical adjustment here is $3G_0$. The photochemical adjustment decays towards the lower stratosphere and troposphere, where the ozone response eventually resembles the prescribed depletion. ~~The~~ By integrating these curves, it is evident that the overall column response of ozone is substantially modified by photochemical adjustment~~, as can be seen by integrating these curves~~. The column integral of the prescribed perturbation is $-G_0 * 60$ km~~. The~~, whereas the column integral of the ~~fully interactive~~ Fully Interactive response is only half as large~~, with the difference due to photochemical adjustment . Overall, photochemistry~~. Thus, photochemical adjustment significantly compensates for the initial perturbation.

The response to uniform stratospheric cooling of $\Delta T = 10$ K is shown in ~~Figure~~ Fig. 4b. The UV-Locked response (blue) is a strict increase in ozone. Cooling approximately rescales ozone by a constant factor, so the ozone response is shaped approximately like the ~~underlying ozone layer. The fully interactive~~ unperturbed ozone profile. The Fully Interactive response (black) differs substantially from the UV-locked response, especially in the lower stratosphere. The maximum increase in ozone is predicted in both cases to occur around 30 km, but the Fully Interactive response is only half that predicted under UV-locking. This discrepancy is due to photochemical adjustment, which is large and stabilizing throughout much of the stratosphere. Below 20 km, ozone is reduced in absolute terms (reverse self-healing). Integrating the column responses, the increase in total column

ozone in the Fully Interactive case is only 43% as large as the increase in UV-locked; again, photochemical adjustment has halved the perturbation compared to in its absence.

A major result of this analysis is that photochemical adjustment is large and significant throughout the ~~entire stratosphere~~stratosphere, and not just in the lower stratosphere where self-healing and reverse self-healing tend to be found. It is important here to distinguish between photochemical adjustment and self-healing/reverse self-healing. We can express the colloquial definition for self-healing or reverse self-healing as follows:

$$\text{(Reverse) self-healing} \equiv \begin{cases} [\mathrm{O_3}]'_{\text{Fully Interactive}}, & \text{if } \mathrm{sign}([\mathrm{O_3}]'_{\text{Fully Interactive}}) \cdot \mathrm{sign}([\mathrm{O_3}]'_{\text{UV-locked}}) < 0 \\ 0, & \text{otherwise} \end{cases}$$

This definition identifies that self-healing or reverse self-healing are given by the ozone perturbation in a ~~fully interactive simulation conditional on that perturbation having the~~ Fully Interactive simulation wherever the ozone anomaly has the opposite sign to what is expected from the imposed perturbation. Expressed this way, it is clear that self-healing and reverse self-healing are not the same as photochemical adjustment (defined in ~~Equation~~ Eq. 2). Indeed, self-healing and reverse self-healing are often just the tip of the iceberg of much larger photochemical stabilization. This is especially clear in the response to stratospheric cooling (~~Figure~~ Fig. 4b), in which the column-integrated reverse self-healing is only 14% as large as the column-integrated photochemical stabilization.

The two main results ~~of our analysis using the Cariolle v2.9 linear ozone model~~ from this analysis of linear ozone models are that (1) photochemical adjustment is destabilizing above 40 km and (2) photochemical adjustment can be large throughout the stratosphere, much greater than implied by conventional self-healing and reverse self-healing. Photochemical destabilization is inconsistent with the standard explanation for self-healing and reverse self-healing, and therefore demands a revision to the conceptual understanding of these ubiquitous phenomena. This new conceptual understanding will also provide quantitative insights.

4 Understanding photochemical adjustment ~~with~~ using the Chapman~~Cycle~~+2 model

The large photochemical destabilization above 40 km and the large photochemical adjustment throughout the stratosphere (not ~~just~~ merely in regions of self-healing or reverse self-healing) both demand a revision to present understanding. New understanding ~~can be~~ is challenging to achieve in ~~a~~ comprehensive chemistry-climate ~~model~~ models with tens of prognostic chemical species undergoing hundreds of reactions. Yet, some basic properties of photochemical adjustment do not depend on this complexity, and are reproducible from simpler models. In particular, the prospect of photochemical destabilization was first raised in Hartmann (1978), who found such behavior ~~above 40 km~~ in a modified version of the Chapman Cycle above 40 km. It is at precisely those altitudes that ~~MOBIDIC also simulates~~ the linear ozone models also simulate photochemical destabilization, suggesting that ~~the Chapman Cycle might hold promise for understanding photochemical adjustmentdespite omitting many chemical processes that are known to be important. Jumping ahead to results, Figure 3 showed that~~ radically simplified photochemical models might support quantitative insights into photochemical adjustment.

We have analyzed photochemical adjustment in such a radically simplified model: the *Chapman+2 model*, which begins with the Chapman Cycle ~~(panel b) reproduces the~~ but then augments it with two chemical reactions representing the generalized damping of ozone from sinks of O and O_3 due to catalytic cycles and transport. The Chapman+2 model is comprehensively introduced in recent work focusing on the structure of the ozone layer (Match et al., 2024), complementing our focus here on sensitivities. The Chapman+2 model was shown in Fig. 3 to reproduce the photochemical regimes from ~~a comprehensive chemistry-climate model (panel a).~~ two chemical transport models. We now explain that calculation and use it to develop physical intuition and quantitative insights into photochemical adjustment.

4.1 Methods: The Chapman~~Cycle +2~~ model

The Chapman Cycle ~~is the textbook model of the ozone layer that explains its gross features, e.g., why the ozone layer is~~ considers the effects of ultraviolet radiation driving photochemical reactions of O, O_2, and O_3 (Chapman, 1930). The Chapman Cycle is the foundational model that first explained how photochemistry could lead to an ozone layer in the stratosphere~~(e.g., Jacob, 1999; Brasseur and Solomon, 2005). The Chapman Cycle considers the photochemical equilibrium obtained when ultraviolet radiation impinges on an atmosphere with oxygen species undergoing the following reactions :~~. Yet, the Chapman Cycle underestimates the ozone sink, which in the tropical stratosphere arises predominantly from catalytic cycles and transport. To restore the leading-order ozone sinks, and in line with rich theories of chemical families for the stratospheric ozone photochemistry (Brasseur and Solomon, 2005), we have augmented the Chapman Cycle with two chemical reactions that represent generalized destruction of O and O_3 by catalytic cycles and transport, as follows:

$$O_2 + h\nu \rightarrow O + O \quad (\lambda < 240 \text{ nm}) \tag{R1}$$

$$O + O_2 + M \rightarrow O_3 + M \tag{R2}$$

$$O_3 + h\nu \rightarrow O_2 + O \quad (\lambda < 3201080 \text{ nm}) \tag{R3}$$

$$O + O_3 \rightarrow 2O_2 \tag{R4}$$

$$O \xrightarrow{z_O} \frac{1}{2}O_2 \tag{R5}$$

$$O_3 \xrightarrow{z_{O_3}} \frac{3}{2}O_2 \tag{R6}$$

where ~~Reactions R1and~~ R1-R4 is the classical Chapman Cycle, and R5-R6 are the two additional generalized sinks. R1 and R3 are photolysis reactions and ~~M~~ M is a third body with the number density of air (n_a). The combination reactions proceed as the number density of the chemical reactants multiplied by a rate coefficient k_i, i=2,4, e.g., reaction 2 has a rate of k_2[O][O_2][M], which in general depends on temperature. The generalized reactions represent two sink pathways: destruction of odd oxygen can scale with atomic oxygen, as in R5 that proceeds at the rate κ_O[O], or it can scale with ozone, as in R6 that proceeds at the rate κ_{O_3}[O_3]. ~~We will now assume that the~~

For typical equilibria of the Chapman Cycle, the molar fraction of O_2 is ~~constant, because it is much larger than the molar fractions of O~~ several orders of magnitude larger than that of O and O_3 ~~or O~~, and will be treated as constant ($C_{O_2} = 0.21$). Under this assumption, these reactions can be ~~manipulated algebraically~~ algebraically solved to yield a quadratic equation for ~~ozone~~ O_3 at a given altitude~~as it depends on the ultraviolet fluxes and collisional reaction rates (Craig, 1965)~~:

$$[\text{O}O_3] = \frac{k_2}{k_4}\frac{J_{O_2}k_2}{k_4}C_{O_2}^2 n_a^2 \frac{k_1 C_{O_2} n_a}{k_1 C_{O_2} n_a + k_3[O_3]}^3 \frac{1}{J_{O_3}[O_3] + J_{O_2}C_{O_2}n_a + \frac{\kappa_{O_3}[O_3]}{2} + \frac{J_{O_3}\kappa_O}{2k_4} + \frac{k_2\kappa_{O_3}C_{O_2}n_a^2}{2k_4} + \frac{\kappa_O\kappa_{O_3}}{2k_4}} \tag{4}$$

~~where the rates of each reaction are indicated k_i (i=1-4), C_{O_2} is the molar fraction of O_2 (0.21), and n_a is the number density of air (molec cm^{-3}). Following a similar derivation , the atomic oxygen can be expressed as a diagnostic function of ozone (Craig, 1965)~~

A similar derivation yields a diagnostic equation for atomic oxygen:

$$[O] = \frac{k_1[O_2] + k_3[O_3]}{k_2 C_{O_2} n_a^2} \frac{J_{O_2}C_{O_2}n_a + J_{O_3}[O_3] + \frac{\kappa_{O_3}[O_3]}{2}}{k_2 C_{O_2} n_a^2 + \frac{\kappa_O}{2}} \tag{5}$$

~~These equations can be simplified for stratospheric conditions. Through much of the stratosphere, the majority of photons are absorbed by ozone compared to O_2, i.e., $k_3[O_3] \gg k_1 C_{O_2} n_a$, leading Equation ?? to simplify to the following standard approximation:~~

$$[O_3] = \left(\frac{k_1 k_2}{k_3 k_4}\right)^{1/2} C_{O_2} n_a^{3/2}$$

Ozone appears implicitly on the right-hand side of ~~Equation ??~~ Eq. 4 through the photolysis rates ~~k_1~~ J_{O_2} (s^{-1}) and ~~k_3~~ J_{O_3} (s^{-1})~~which are~~ . Photolysis is governed by the spectrally-integrated ~~ultraviolet~~ UV absorption:

$$k_1 J_{O_2}(z) = \int_\lambda q_{O_2}(\lambda)\sigma_{O_2}(\lambda)I_\lambda(z)d\lambda \tag{6}$$

$$k_3 J_{O_3}(z) = \int_\lambda q_{O_3}(\lambda)\sigma_{O_3}(\lambda)I_\lambda(z)d\lambda \tag{7}$$

with wavelength λ, quantum yield $q_i(\lambda)$ (molecules decomposed per photon absorbed by species i), absorption coefficient σ_i (cm^2 molec^{-1}) ~~shown in Figure 5, and actinic~~ (Fig. 5b), and UV flux density with respect to wavelength $I_\lambda(z)$ (photons cm^{-2} s^{-1} nm^{-1}) . The absorption of photons by photolysis attenuates the ~~actinic~~ UV flux:

$$I_\lambda(z) = I_\lambda(\infty)\exp\left(-\frac{\tau_\lambda(z)}{\cos\theta}\right) \tag{8}$$

where $I_\lambda(\infty)$ is the incoming ~~actinic flux~~ UV flux (Fig. 5a), θ is the solar zenith angle, and τ_λ is the optical depth as a function of wavelength. The optical depth at a given altitude depends on column-integrated O_2 and O_3 above that level:

$$\tau_\lambda(z) = \sigma_{O_2}(\lambda)\chi_{O_2}(z) + \sigma_{O_3}(\lambda)\chi_{O_3}(z) \quad (9)$$

where $\chi_{O_2} = \int_z^\infty [O_2]dz$ and $\chi_{O_3} = \int_z^\infty [O_3]dz$.

4.1.1 ~~Chapman Cycle numerics~~

The collisional reaction rates k_2 and k_4 are calculated with temperature-dependent values from Brasseur and Solomon (2005). The generalized sinks of O and O_3 proceed with damping rates representing both transport and catalytic cycles. Motivated by consideration of the tropical lower stratosphere, in which upwelling advects ozone-poor air up from below in order to damp O_3 (e.g., Match and Gerber, 2022), transport will be crudely parameterized as a constant damping of $\kappa_{\bar{w}^*}$ = (3 months)$^{-1}$. Catalytic cycles will be parameterized by taking all (temperature-dependent) damping-like terms from the budget of generalized odd oxygen (O_y) of Brasseur and Solomon (2005), i.e., terms of the form $\partial O_y/\partial t = -k[Z_O][O]$ are taken to damp O, and terms of the form $\partial O_y/\partial t = -k[Z_{O_3}][O_3]$ are taken to damp O_3, for catalysts Z_O and Z_{O_3}. This leads to the following damping rates:

~~We use a modified version of the Chapman implementation described in Match and Gerber (2022) in photochemical equilibrium mode with an~~

$$\kappa_O = \kappa_{\bar{w}^*} + a_5[OH] + a_7[HO_2] + 2b_3[NO_2] + 2d_3[ClO] + 2e_3[BrO] \quad (10)$$

$$\kappa_{O_3} = \kappa_{\bar{w}^*} + a_2[H] + a_6[OH] + a_{6b}[HO_2] \quad (11)$$

The vertical profile of these damping rates is shown in Fig. 5c. To validate these damping rates, we also show the odd oxygen damping timescale from the Cariolle v2.9 linear ozone model compared to the equivalent timescale implied in the Chapman+2 model (cyan curves). The chemical reactions that comprise the damping in the Chapman+2 model are intended to provide only an idealized representation of the global stratosphere, while excluding photochemical reactions among the catalysts, heterogeneous chemistry in the polar stratosphere, and tropospheric chemistry. The simplified representation of transport is intended to provide an idealized representation of only the tropical lower stratosphere. These geographical caveats will be considered when using the Chapman+2 model to interpret the global results from the linear ozone models.

4.2 Chapman+2 model numerics

We use the Chapman+2 model as implemented in Match et al. (2024). This solution is solved for a steady-state, isothermal atmosphere and a default of overhead sun ($\cos\theta = 1$). We neglect ~~transport, tropospheric chemistry,~~ scattering, clouds, and

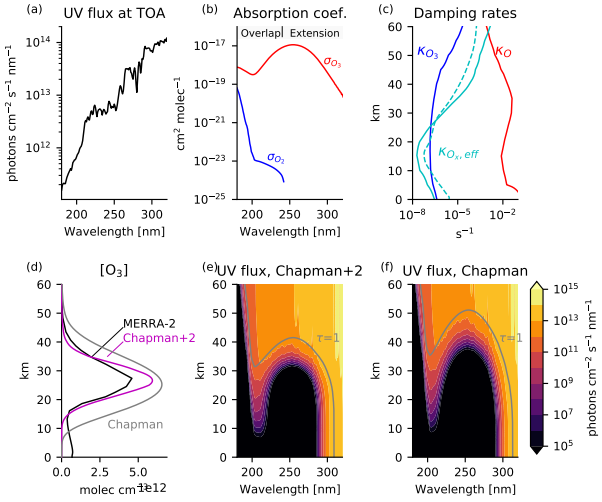

Figure 5. ~~Basic state of~~ Boundary conditions and solutions to the Chapman+2 model. (a) ~~Actinic~~ UV flux at the top of the atmosphere. (b) Absorption coefficients for O_2 and O_3. (c) ~~Chapman~~ Generalized damping rates of O (red) and O_3 ~~profile~~ (~~black~~blue) ~~versus MERRA-2~~ estimated from Eqs. 10 and 11, using catalyst profiles from the chemistry-climate model SOCRATES, as tabulated in Brasseur and Solomon (2005). The effective damping rate of O_x (solid cyan) is comparable to the derived O_3 relaxation rate in the Cariolle v2.9 linear ozone model (dashed cyan). (d) Ozone profiles in the Chapman Cycle (gray) and Chapman+2 model (magenta) compared to the O_3 profile averaged from 30°S-30°N in 2018 in the Modern Era Retrospective analysis for Research and Applications Version 2 (~~magenta~~MERRA-2), which blends direct observations with a state-of-the-art atmosphere model to provide a state estimate of the atmosphere (black). (~~d~~e) ~~Actinic~~ UV flux ~~in~~ for the Chapman+2 model ~~resolved~~ and (f) the Chapman Cycle, indicating the level of unit optical depth ($\tau(\lambda) = 1$) in gray. For clarity, wavelength ~~and altitude~~axes are restricted to 180-320 nm although the numerical solution extends up to 800 nm in the weakly-absorbing Chappuis bands.

surface reflection. ~~Equation ??~~ Eq. 4 is solved at each altitude downward from the top of the atmosphere to calculate the photochemical equilibrium profile~~(Craig, 1965; Ratner and Walker, 1972)~~.

The vertical dimension is discretized into vertical levels ($\Delta z = 100$ meters) ranging from the surface to 100 km. The idealized shortwave radiative transfer and photolysis rates are solved on a wavelength grid with ~~141~~ 621 discretized wavelengths ranging from 180 nm to ~~320~~ 800 nm. Spectrally-resolved parameters are linearly interpolated to the wavelength grid. Solar ~~actinic~~ UV flux is calculated from the Solar Spectral Irradiance Climate Data Record (Coddington et al., 2015), averaged from 01-01-2020 to 02-04-2021. O_2 absorption coefficients (σ_{O_2}) are taken from Ackerman (1971) and O_3 absorption coefficients (σ_{O_3}) from ~~Demore et al. (1997)~~Sander et al. (2010). The isothermal atmosphere has a default temperature of 240 K and scale height of 7 km. Temperature-dependent parameters for reaction rates $k_2(T)$ and $k_4(T)$ are taken from Brasseur and Solomon (2005).

~~Chapman photochemical~~ The Chapman+2 model equilibrium is calculated numerically~~. The parameters and resulting photochemical equilibrium are shown in Figure 5. Figure 5c~~, with results shown in Fig. 5. Fig. 5d shows the Chapman Cycle photochemical equilibrium profile of ozone (~~black~~gray) compared to the ~~tropical-averaged~~ Chapman+2 solution (magenta) and a

tropically-averaged profile in MERRA-2 for the representative year of 2018 (~~magenta). Chapman photochemical equilibrium~~ black). The Chapman Cycle is well known to overestimate ozone~~by approximately a factor of two because it neglects~~ , but this overestimate is partially mitigated in the Chapman+2 model by representing sinks from transport and catalytic ~~ozone destruction (Bates and Nicolet, 1950; Crutzen, 1970; Jacob, 1999; Brasseur and Solomon, 2005). Figure 5d shows the actinic~~ cycles (Bates and Nicolet, 1950; Crutzen, 1970; Jacob, 1999; Brasseur and Solomon, 2005). Figs. 5e,f show the UV flux as a function of wavelength and altitude in the ~~photochemical~~ equilibrium solution, with a contour indicating the $\tau = 1$ level where the ~~actinic flux~~ UV flux at a given wavelength has been attenuated by a factor of e compared to the top-of-atmosphere ~~actinic~~ UV flux.

4.3 Photochemical regimes in the Chapman+2 model

~~Conceptually, the photochemical~~ Photochemical regimes in the Chapman~~Cycle are controlled by the relative sensitivity of photolysis of O_2 and photolysis of O~~+2 model are calculated by first formulating the net production rate $(P - L)$ of odd oxygen:

$$P - L = 2J_{O_2}[O_2] - 2k_4[O][O_3] - \kappa_{O_3}[O_3] - \kappa_O[O] \tag{12}$$

This net production rate depends on overhead column O_3 through the UV fluxes, which determine the local photolysis rates. This sensitivity of the photolysis rates to perturbations in ~~column ozone. In response to perturbations in column ozone, photochemical stabilization occurs where the photolytic source of ozone is more sensitive than the photolytic sink; destabilization occurs where the photolytic sink of ozone is more sensitive than the photolytic source. Of course, photolysis of O~~overhead column O_3 ~~acts as a sink of ozone with an efficiency inversely related to the strength of the null cycle R3 $\rightleftharpoons$ R2. A quantitative calculation of the photochemical sensitivity of the Chapman Cycle must take this null cycle into account.~~ can be calculated by differentiating Eqs. 6 and 7 with respect to χ_{O_3}, yielding a factor of $-\sigma_{O_3}(\lambda)/\cos\theta$:

$$\frac{\partial J_{O_2}}{\partial \chi_{O_3}} = -\int_\lambda q_{O_2}(\lambda)\sigma_{O_2}(\lambda)\overline{I_\lambda}(z)\left(\frac{\sigma_{O_3}(\lambda)}{\cos\theta}\right)d\lambda \tag{13}$$

$$\frac{\partial J_{O_3}}{\partial \chi_{O_3}} = -\int_\lambda q_{O_3}(\lambda)\sigma_{O_3}(\lambda)\overline{I_\lambda}(z)\left(\frac{\sigma_{O_3}(\lambda)}{\cos\theta}\right)d\lambda \tag{14}$$

where $\overline{I_\lambda}(z)$ is the basic state UV flux. The photochemical sensitivities in Eqs. 13 and 14 are strictly negative, confirming that increasing overhead column ozone can only reduce photolysis rates by attenuating the UV flux.

~~We calculate the photochemical sensitivity by quantifying how the~~

The overall photochemical sensitivity of the Chapman+2 model is calculated as $\partial(P - L)/\partial\chi_{O_3}$. Of course, in equilibrium the net production rate ~~of ozone (source minus sink) changes~~ is zero, suggesting that no perturbation can modify $P - L$.

However, the photochemical sensitivity considers a situation that is out of equilibrium, insofar as it asks: in response to a perturbation in ~~column ozone while holding ozone itself locally fixed. (Holding ozone fixed is essential, because if ozone was allowed to adjust, then photochemical equilibrium would prevail and the source would necessarily balance the sink in both the control and perturbed states.) The~~ overhead column O_3 that leads to a local perturbation in UV fluxes, would the net production rate of ozone ~~in the Chapman Cycle comes from R2, R3, and R4:~~

$$P - L = k_2[\mathrm{O}][\mathrm{O_2}][M] - k_3[\mathrm{O_3}] - k_4[\mathrm{O}][\mathrm{O_3}]$$

~~Substituting in the expression for atomic oxygen (Equation **??**) leads to the following expansion of the net production rate after grouping terms by their dependence on k_1 versus k_3:~~

$$P - L = k_1[\mathrm{O_2}](1-\epsilon) - \epsilon k_3[\mathrm{O_3}]$$

~~where $\epsilon \equiv k_4[\mathrm{O_3}]/k_2 C_{\mathrm{O_2}} n_a^2$ indicates the destruction efficiency with which photolysis of ozone leads to the destruction of ozone, and can be seen to equal the the rate of R4 (by which atomic oxygen destroys ozone) divided by the rate of R2 (by which atomic oxygen produces ozone). Photolysis of ozone (k_3)evidently acts as a loss of ozone because it appears exclusively in a negative term. However, this sink of ozone is not one-to-one with the photolysis events, because much photolysis of O~~tend to increase or decrease? In other words, the photochemical sensitivity is calculated by perturbing overhead column O_3 ~~drives the null cycle from R3 to R2. At 35 km, $\epsilon \sim O(10^{-3})$, meaning that out of 1000 photolysis events of ozone, 999 will proceed into the null cycle and only 1 will actually turn the odd oxygen back into O_2~~but keeping local ozone fixed (and therefore out of equilibrium). ~~The strength of the null cycle $(1-\epsilon)$ also modulates the effectiveness of photolysis of O_2 at producing ozone. If the null cycle is weak such that atomic oxygen tends to destroy ozone, then photolysis of O_2 would not be as strong a source of ozone. The smallness of ϵ (i.e., $\epsilon < 1$) guarantees that photolysis of O_2 is always a source of ozone.~~

~~Holding ozone fixed at its control value of~~ We calculate this photochemical sensitivity beginning with Eq. 12, substituting in the expression for atomic oxygen (Eq. 5), then differentiating with respect to column O_3 while holding O_3 fixed (at $\overline{[\mathrm{O_3}]}$~~, we can differentiate Equation 15 with respect to column ozone, where the only terms that depend on column ozone are the photolysis rates k_1 and k_3:~~), yielding:

$$\frac{\partial(P-L)}{\partial \chi_{\mathrm{O_3}}} = \frac{\partial k_1}{\partial \chi_{\mathrm{O_3}}}[\mathrm{O_2}](1-\epsilon) - \epsilon \frac{\partial k_3}{\partial \chi_{\mathrm{O_3}}}\overline{[\mathrm{O_3}]}$$

$$\partial \chi_{\mathrm{O_3}} \approx \frac{\partial J_{\mathrm{O_2}}}{\partial \chi_{\mathrm{O_3}}}[\mathrm{O_2}](1-\epsilon) - \epsilon \frac{\partial J_{\mathrm{O_3}}}{\partial \chi_{\mathrm{O_3}}}\overline{[\mathrm{O_3}]} \quad (15)$$

The ozone layer is photochemically stabilizing when $\frac{\partial(P-L)}{\partial\chi_{O_3}} < 0$ ~~and photochemically destabilizing when $\frac{\partial(P-L)}{\partial\chi_{O_3}} > 0$.~~ ~~The destruction efficiency~~, indicating that an increase in overhead column ozone leads to a reduction in net photochemical production. The ozone layer is photochemically destabilizing when $\frac{\partial(P-L)}{\partial\chi_{O_3}} > 0$. When considering the photochemical sensitivity from Eq. 15, recall that $\partial J_{O_2}/\partial\chi_{O_3} < 0$ and $\partial J_{O_3}/\partial\chi_{O_3} < 0$ (Eqs. 13 and 14), because increasing overhead column O_3 reduces photolysis rates. The sensitivities of the photolytic source and sink are weighted by the leakage from the null cycle R2⇌R3, ϵ ~~can be calculated from the basic state solution of ozone and actinic fluxes. It turns out that the partial derivatives of the photolysis rates to perturbations in column ozone can also be calculated explicitly by noting that photolysis rates depend on column ozone through the term $\exp(-\sigma_{O_3}(\lambda)\chi_{O_3}/\cos\theta)$, which can be differentiated with respect to χ_{O_3} to yield a factor of $-\sigma_{O_3}(\lambda)/\cos\theta$. The resulting sensitivities (i. e.~~, which measures the strength of the photolytic sink. When ϵ is zero, there is no photolytic sink of odd oxygen, leading to strict photochemical stabilization ($\frac{\partial(P-L)}{\partial\chi_{O_3}} < 0$). When $\epsilon > 0$, there is a photolytic sink of odd oxygen from some combination of the Chapman sink (captured in the term $k_4[\overline{O_3}]$) and the damping of atomic oxygen (captured in the term $\kappa_O/2$), and photochemical destabilization becomes possible, although not guaranteed. The leakage itself is small; for example, at 45 km, $\epsilon \sim O(10^{-2})$, meaning that out of 100 photolysis events of ozone, ~~the partial derivatives of Equations 6 and 7 with respect to column ozone) are as follows:~~ 99 will proceed into the null cycle and only 1 will leak into a sink of odd oxygen. However, photochemical destabilization nonetheless occurs at this altitude because J_{O_3} at 45 km is six orders of magnitude more sensitive to perturbations in overhead column O_3 than is J_{O_2}.

$$\frac{\partial k_1}{\partial\chi_{O_3}} = -\int_\lambda q_{O_2}(\lambda)\sigma_{O_2}(\lambda)\overline{I_\lambda}(z)\left(\frac{\sigma_{O_3}(\lambda)}{\cos\theta}\right)d\lambda$$

$$\frac{\partial k_3}{\partial\chi_{O_3}} = -\int_\lambda q_{O_3}(\lambda)\sigma_{O_3}(\lambda)\overline{I_\lambda}(z)\left(\frac{\sigma_{O_3}(\lambda)}{\cos\theta}\right)d\lambda$$

~~where $\overline{I_\lambda}(z)$ is the basic state actinic flux. Equations 13 and 14 are strictly negative, confirming that increasing column ozone can only reduce photolysis ratesby attenuating the actinic flux. Evaluating Equations 13 and 14 only requires variables diagnosed from the basic state (e. g., the basic state actinic flux) and integrals with respect to wavelength. Importantly, Equations 13 and 14 are not mathematically implicit (i. e., perturbation ozonedoes not appear implicitly on the right-hand-side) and do not require an iterative integral in altitude. Thus, Equations 13 and 14 can be substituted into Equation **??** to yield an explicit formula for the sensitivity of the ozone net production rate to perturbations in column ozone in terms of only local properties of the ozone layer and basic state variables.~~

~~This explicitly-calculated~~

Explicit calculations of the photochemical sensitivity of the Chapman~~Cycle is shown in Figure 3b~~+2 model are shown in Fig. 3c. The solar zenith angle has been approximated ~~as the latitude~~ by the latitude (neglecting the diurnal cycle) to allow a global column-by-column comparison with the photochemical sensitivity of ~~MOBIDIC~~ the linear ozone models during the equinoctial month of March (~~Figure 3a~~Figs. 3a,b). The Chapman~~Cycle~~ +2 model reproduces the gross features of ~~MOBIDIC~~the

linear ozone models, most importantly the destabilizing regime above 40 km in the tropics and the stabilizing regime below. The ChapmanCycle +2 model reproduces the latitudinal dependence in which the transition between the destabilizing regime and the stabilizing regime shifts up to higher altitudes at higher latitudes.

Interpreting Equation ??, it is evident that the conventional explanation for self-healing, which assumes that photolysis is As a caveat, the representation of transport-based damping of O_3 in the Chapman+2 model is not designed to represent the extratropics, for which transport is generally a source of ozone, neglects the . However, transport only enters indirectly into the photochemical sensitivity of the ozone sink ($\partial k_3/\partial \chi_{O_3}$). The full ChapmanCycle analysis reveals that the photochemical sensitivity of the ozone layer is controlled by the relative magnitudes of the sensitivity of k_1 and k_3 (the latter being weighted by the destruction efficiency). Equations 13 and 14 indicate that the sensitivities of the photolysis rates are controlled by the covariance between the spectrally-resolved photolysis rate in the basic state and the absorption coefficient of ozone. This presages that the spectral structure of the ozone absorption coefficients will critically control the photochemical sensitivity, a theme that we will return to in Section 5. For now, we proceed to a calculation of the full profile of photochemical adjustment in the Chapman CycleChapman+2 model through its effects on the basic state ozone, with κ_{O_3} not appearing explicitly in Eqs. 15 and ??, so these results are not expected to be overly sensitive to the unrealistic aspects of transport.

4.4 Photochemical adjustment in the Chapman Cycle

As with MOBIDIC, we

4.4 Photochemical adjustment in the Chapman+2 model

We calculate the photochemical adjustment of the ChapmanCycle in +2 model in the tropical stratosphere in response to ozone depletion and cooling, considering the same perturbations as analyzed for the Cariolle v2.9 linear ozone model. It is not trivial to drive a vertically uniform loss of ozone in a fully interactive system, even one this simple, due to the vertical coupling through the actinic flux. The effect of ozone UV flux. Ozone depletion is therefore constructed imposed with an iterative calculation of ozone and overhead column ozone, working from the top of the atmosphere downwards. Starting at the uppermost level, we first compute the equilibrium [O_3], and then overwrite it with our ozone loss perturbation, [O_3]-G_0. At the next level down, we can then compute the equilibrium [O_3], where the photolysis rates depend on the perturbed ozone column above. Again, this is overwritten with the imposed loss: [O_3]-G_0, and the calculation proceeds iteratively downwards yielding an ozone profile with a uniform deficit of ozone, but otherwise consistent with the actinic UV flux. Stratospheric cooling is comparatively more straightforward to implement, incorporated through the temperature dependence of the collisional rates k_2 and k_4 and of the generalized damping rates (Eqs. 10 and 11), using the functions for temperature dependence from Brasseur and Solomon (2005). The Chapman+2 model is designed to represent photochemistry in the stratosphere but not the troposphere, so while full profiles are shown down to the surface in order to provide a complete characterization of the stratospheric regime, these should not be considered to represent the true response in the troposphere.

The UV-locked experiment is performed by locking both k_1 and k_3 J_{O_2} and J_{O_3} to their control profiles. More refined photolysis-locking is also possible in the ChapmanCycle+2 model, because we can separately lock k_1 or k_3 J_{O_2} or J_{O_3}. This

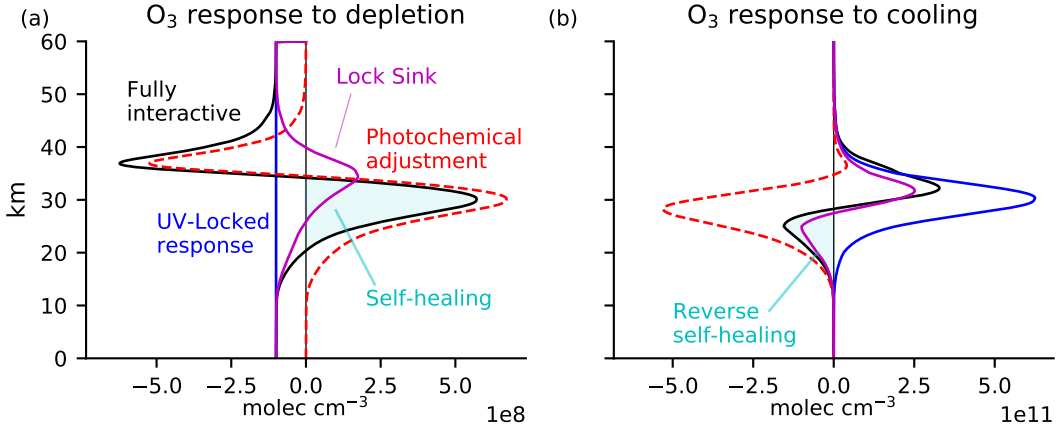

Figure 6. The Chapman~~Cycle~~ +2 model response to the same perturbations as in ~~Figure~~ Fig. 4, i.e. (a) ozone depletion by 10^8 molec cm^{-3} everywhere below 60 km and (b) uniform cooling of 10 K. The Chapman~~Cycle~~ +2 model reproduces the response structure calculated using the Cariolle v2.9 linear ~~emulator of MOBIDIC~~ozone model. The Chapman~~Cycle~~ +2 model also permits the calculation of a Lock Sink response (magenta), for which only ~~k_3~~ J_{O_3} was locked while ~~k_1~~ J_{O_2} was allowed to adjust to the overhead ozone, emulating the conventional explanation for self-healing and reverse self-healing, yet failing to reproduce key aspects of the ~~ozone~~ Fully Interactive response~~to perturbations~~.

allows us to test the prevailing explanation for the response of the ozone layer to perturbations, which neglects the sensitivity of the ozone sink (~~k_3) to~~ J_{O_3}) to overhead column ozone perturbations. We perform Lock Sink experiments in which ~~k_3~~ J_{O_3} is locked, quantitatively enforcing this common assumption to test whether it reproduces the Fully Interactive response.

The results for ~~quantifying photochemical adjustment in the Chapman Cycle in response to~~ ozone depletion and cooling are shown in ~~Figure~~ Fig. 6. These results reproduce the key structure of those from the ~~linear emulator of MOBIDIC in Figure~~ Cariolle v2.9 linear ozone model in Fig. 4, including our two major results: (1) photochemical adjustment is destabilizing above 40 km and (2) photochemical adjustment is large throughout the stratosphere, with self-healing and reverse self-healing often just the tip of the iceberg.

The Lock Sink experiments provide a unique result from the Chapman~~Cycle experiments~~+2 model, which could not be performed in the linear ~~emulator of MOBIDIC~~ ozone model (because it did not distinguish between the ~~ozone~~ photolytic source and sink). If the prevailing explanation for photochemical adjustment ~~applies~~ applied to the Chapman~~Cycle~~+2 model, then photochemical adjustment would be ~~dominated~~ driven by changes in ~~the ozone source~~ J_{O_2} with minimal contributions from changes in ~~the ozone sink~~ J_{O_3}. Thus, the prevailing explanation for photochemical adjustment can be quantitatively tested by comparing the Lock Sink experiment (magenta) against the Fully Interactive experiment (black). This comparison reveals major limitations in the prevailing explanation. ~~By construction, the Lock Sink experiments cannot produce photochemical destabilization, because photochemical destabilization occurs when the sink is more sensitive than the source.~~ Because it cannot produce photochemical destabilization, the Lock Sink experiment fails to predict the large self-amplified destruction

above 40 km in response to ozone depletion. Around ~~45~~ 40 km in the Fully Interactive experiment, the contribution from self-amplified destruction actually exceeds the local magnitude of G_0, leading to absolute reductions of ozone exceeding $2G_0$. At these levels of maximum self-amplified destruction, the Lock Sink experiment wrongly predicts photochemical stabilization. ~~The substantial self-healing~~ Self-healing is therefore biased towards higher altitudes in the Lock Sink experiment compared to in the Fully Interactive experiment.

~~In the Cooling experiment, the response under UV-Locking is a rescaling of the ozone layer by a constant factor. (In the linear emulator of MOBIDIC, the response is not strictly a rescaling because the background state is not isothermal, ozone is not in photochemical equilibrium, and other processes beyond the Chapman Cycle are represented; the overall response to cooling has a similar shape to the Chapman Cycle solution but smaller magnitude.)~~ Under cooling, ozone generally increases due to changes in the collisional reaction rates. This is reflected in the predicted response under UV-locking (Fig. 6b, blue). Of course, these increases in ozone then induce photochemical adjustment. In both the Chapman~~Cycle and the linear emulator of MOBIDIC~~+2 model and the Cariolle v2.9 linear ozone model, the *Fully Interactive* response of the ozone layer ~~quickly deviates from the direct temperature responsedue to~~ already deviates at high altitudes from the UV-locked response, reflecting this photochemical adjustment (Fig. 6b, red dashed curve). Photochemical adjustment generally stabilizes the ozone layer in response to cooling, although there is subtle destabilization ~~, again~~ above 40 km. Reverse self-healing, in which ozone is reduced in *Fully Interactive* compared to *Control* (negative values of the black curve), is generally considered to be the primary manifestation of photochemical stabilization. Yet, reverse self-healing only captures a sliver of the much-larger photochemical stabilization (negative values of the red curve). ~~Reverse self-healing is stronger in the Off-Line Cariolle v2.9 emulator than in the Chapman Cycle, suggesting arole for non-Chapman stabilizing processes including catalytic chemistry and transport (Wuebbles et al., 1983; Solomon et al., 1985; WMO, 1985)~~Interestingly, the Lock Sink calculation better reproduces the ozone response to cooling (Fig. 6b) than to depletion (Fig. 6a).

5 A spectral interpretation of photochemical stabilization and destabilization

~~Ozone depletion and cooling caused both photochemical destabilization and photochemical stabilization, with the ChapmanCycle and linear emulator of MOBIDIC both simulating a~~ The linear ozone models and Chapman+2 model robustly agree on the altitude of the photochemical regime transition from destabilization aloft to stabilization below~~around 40 km in the tropics. Analysis of the Chapman Cycle reveals that~~ . Thus, this regime transition is likely explained by simple physics that is shared among these models. Indeed, we find that the regime transition is controlled by which parts of the absorption spectrum for O_3 and O_2 have been attenuated versus which parts of the absorption spectrum are still active. ~~Recall that absorption of photons by O_2 drives the production of O_3, whereas absorption of photons by O_3 drives the destruction of O_3.~~ Two key spectral windows will turn out to determine the overall photochemical regime: (1) the *overlap window*, which has absorption by both O_2 and O_3, occurring for $\lambda < 240$ nm, and (2) the *extension window*, which has absorption by only O_3, occurring for $\lambda > 240$ nm. These absorption spectra are shown in ~~Figure~~ Fig. 5b.

~~Photochemical stabilization can only occur in the overlap window where photons can~~

The overlap window can produce either photochemical stabilization, where photons switch between being absorbed by O_2 and O_3 ~~. The overlap window can also support photochemical destabilization~~(e.g., Crutzen, 1974), or photochemical destabilization, where photons are absorbed by O_3 in both the control and perturbed cases. The extension window can only support photochemical destabilization~~. The relative importance~~ , because photons must be absorbed by O_3 in both cases. Thus, the photochemical sensitivity is determined by the relative sensitivity of absorption in these two ~~spectral windows turns out to be dominantly~~ windows to perturbations in overhead column O_3. This relative sensitivity is in turn controlled by a single variable endogenous to the ozone ~~dynamics: column ozone. Under the control of column ozone, the photochemical regimesemerge as follows~~dynamics—overhead column ozone—leading to the following photochemical regimes:

- **Photochemically neutral regime**: When overhead column ozone is so small that the ozone layer is optically thin at all wavelengths, absorption in both windows varies linearly with overhead column ozone, and the ozone layer is photochemically neutral.

- **Photochemically destabilizing regime**: As overhead column ozone increases, the first wavelength to saturate with respect to absorption by ozone (i.e., exceed $\tau_{O_3} \approx 1$) occurs at the peak absorption coefficients of ozone of $\sigma_{O_3} \approx 10^{-17}$ cm^2 $molec^{-1}$ ~~.~~(Fig. 6b). Unit optical depth is thus first reached for ~~a~~ an overhead column ozone of $\chi_{O_3} = 1/\sigma_{O_3,max} \approx 10^{17}$ molec cm^{-2}. The wavelengths where absorption first saturates are ~~at the center of the~~ in the Hartley band, ~~which is~~ centered in the extension window. Therefore, at these overhead column ozone values, absorption in the extension window is more sensitive to perturbations in overhead column ozone than is absorption in the overlap window, which remains optically unsaturated. Because absorption in the extension window is by ozone only, this means that the ozone sink is more sensitive to perturbations in overhead column ozone than the ozone source, a destabilizing regime.

- **Photochemically stabilizing regime**: As overhead column ozone increases further, the overlap window ~~saturates around a~~ optically saturates around an overhead column ozone of 10^{18} molec cm^{-2}. Beyond this overhead column ozone threshold, the ozone source in the overlap window attenuates exponentially as a function of overhead column ozone, whereas the ozone sink in the extension window still has some unsaturated wavelengths that attenuate linearly as a function of overhead column ozone. Thus, absorption in the overlap window becomes more sensitive than in the extension window, stabilizing the ozone layer.

The ~~destabilization layer robustly terminates at~~ bottom of the destabilization layer occurs robustly around 40 km ~~in response to diverse perturbations~~ because that is where overhead column ozone surpasses the stabilization threshold of 10^{18} molec cm^{-2}. These overhead column ozone thresholds have been validated with mechanism denial experiments using the Chapman~~Cycle~~+2 model. For example, we flattened the absorption coefficients in the overlap window and then artificially varied ~~their magnitudes across three~~ them across two orders of magnitude. As expected, destabilization initiates once the peak absorption of the Hartley band saturates, and stabilization initiates once the overlap window saturates, as shown in Fig. 7. ~~Figure 7shows these results.~~ Thus, if the overlap window is forced to have an absorption coefficient comparable to the peak absorption of the Hartley band, then destabilization vanishes (Fig. 7d).

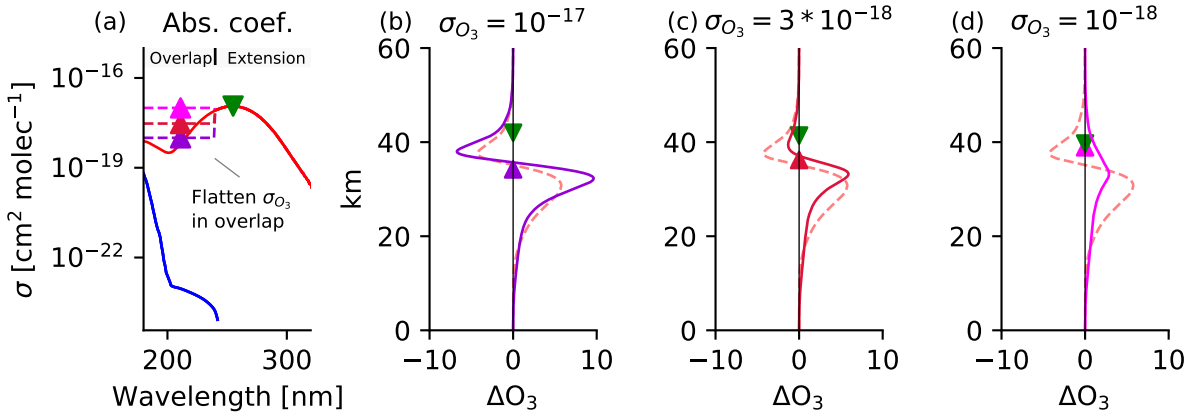

Figure 7. Photochemical adjustment in the Chapman+2 model in response to uniform ozone depletion under different constant values of σ_{O_3} in the overlap window. (a) The absorption spectra where σ_{O_3} in the overlap window is flattened at various constant values. (b-d) For each constant ~~values~~ value of σ_{O_3}, (normalized) photochemical adjustment is calculated in response to uniform ozone depletion of $G_0 = 10^8$ molec cm^{-3} below 60 km~~, normalized by dividing by G_0~~. Spectral theory (Section 5) correctly predicts that destabilization ($\Delta O_3 < 0$) begins at the overhead column ozone threshold where the extension window begins to saturate (green downward-pointing triangle). Spectral theory also correctly predicts the transition from destabilization to stabilization at the overhead column ozone threshold where the overlap window saturates (upward-pointing triangles), which varies across the three experiments. If the top and bottom of the destabilization regime occur at the same altitude, then the destabilization regime vanishes (panel d). Photochemical adjustment using the true absorption coefficients ~~(as seen in Figure 6a)~~ is plotted as the red dashed curve (identical in panels b-d, and as plotted in Fig. 6a).

~~These column ozone thresholds have been validated for the linear ozone model coefficients calculated from MOBIDIC. Figure~~ The principle that destabilization occurs where the overlap window is optically unsaturated has been validated in the Cariolle v2.9 and LINOZ linear ozone models. Fig. 3 includes magenta curves corresponding to the slant overhead column ozone threshold of 10^{18} molec cm^{-2}, where slant overhead column ozone has been calculated as $\chi_{O_3}/\cos(\theta)$ with θ taken as the latitude (noting that we chose an equinoctial month to approximately equate latitude with zenith angle, although neglecting the diurnal cycle in sun angle). In ~~MOBIDIC~~the linear ozone models, the climatological overhead column ozone is given by parameter A_7, and in the Chapman~~Cycle~~+2 model, the climatological ozone is calculated ~~as the photochemical equilibrium profile~~ at each latitude, approximating θ with latitude. Although ~~not perfect~~imperfect, the theoretical curve approximately reproduces the transition from destabilization to stabilization, including its latitudinal structure (~~Figure~~ Fig. 3). At high latitudes, the transition from destabilization to stabilization occurs at a higher altitude due to the oblique angle of the sunlight, which reaches the slant overhead column ozone threshold more rapidly for a given ozone profile.

6 Updating the explanation for self-healing and reverse self-healing

Photochemical models produce photochemical adjustment as a natural consequence of accurately representing photochemistry. Thus, the key results of this paper are primarily conceptual, since they inform how the sensitivity of the ozone layer to perturbations is interpreted and explained. These results could also have implications for certain decisions made when formulating photochemical models, considered in the Discussion. However, the main conceptual advances from this paper suggest that some of the previous explanations of ozone self-healing and reverse self-healing could ~~lead readers to develop a distorted view~~ distort understanding of photochemical adjustment.

Most explanations suggest that self-healing and reverse self-healing can be understood by considering the effect of the perturbed ultraviolet fluxes on the photolytic ozone source. For example, self-healing is explained in Hudson (1977) as follows: "O_3 destruction at the upper levels in the stratosphere is partially compensated by the increase in O_3 at the lower levels due to deeper penetration of solar UV radiation." Similarly, in one of the few textbook explanations of self-healing, Finlayson-Pitts and Pitts (2000) wrote: "When stratospheric O_3 is removed... there is more light available for photolysis of ~~O2~~ O_2 and the formation of more ozone." Although not strictly wrong, these explanations might lead to the incorrect impression that deeper penetration of solar UV radiation generally leads to increased ozone. Instead, we have shown that this common explanation ~~applies only to~~ only gives correct intuition for the stabilizing regime of ozone photochemistry, but ~~that there is also a destabilizing regimeof ozone photochemistry~~not the destabilizing regime. Photochemical adjustment cannot generally be understood by only considering the effects of the perturbation ultraviolet flux on the ozone source. Neglecting the effects of the perturbation ultraviolet flux on the ozone sink was shown to lead to errors in the magnitude and vertical structure of the photochemical adjustment (~~Figure~~ Fig. 6).

Thus, it seems plausible to formulate a minimal explanation for self-healing and reverse self-healing~~that is consistent with the reality of photochemical adjustment with reference to a basic state in photochemical equilibrium. Thus, we explain ozone self-healing and reverse self-healing~~ , as follows:

- **Self-healing:** Ozone depletion enhances ultraviolet fluxes penetrating to lower altitudes, increasing both the ozone source and the ozone sink. Ozone ~~can exhibit~~ exhibits a local net increase (self-healing) if the photolytic ozone source increases more than the photolytic ozone sink, and that increase is large enough to overcome any local ozone depletion.

- **Reverse self-healing:** Ozone enhancement reduces ultraviolet fluxes penetrating to lower altitudes, reducing both the ozone source and the ozone sink. Ozone ~~can exhibit~~ exhibits a local net decrease (reverse self-healing) if the photolytic ozone source decreases more than the photolytic ozone sink and that decrease is large enough to overcome any local ozone enhancement.

7 Discussion

7.1 Sink regimes of the Chapman+2 model

The photolytic sink of O_3, resulting from leakage out of the null cycle R2⇌R3, is in some places the dominant sink of O_3, but is not dominant everywhere. Where the photolytic sink is not the dominant sink of O_3, modulation of the photolytic sink by photochemical adjustment is not expected to be as significant in determining O_3. Match et al. (2024) analyzed limiting cases of the Chapman+2 model in which each of its three sinks of odd oxygen dominate: the Chapman Cycle sink limit (R4), the O-damped limit (R5), and the O_3-damped limit (R6). When these limits are strictly satisfied and under other realistic assumptions such as that O_3 is the dominant absorber of UV, these limits lead to the following distinct scaling relationships for the ozone profile with altitude:

$$[O_3]_{\text{Chapman}} = \left(\frac{J_{O_2} k_2}{J_{O_3} k_4}\right)^{1/2} C_{O_2} n_a^{3/2} \tag{17}$$

$$[O_3]_{\text{O-damped}} = \frac{2 J_{O_2} k_2 C_{O_2}^2 n_a^3}{J_{O_3} \kappa_O} \tag{18}$$

$$[O_3]_{O_3\text{-damped}} = \frac{2 J_{O_2} C_{O_2} n_a}{\kappa_{O_3}} \tag{19}$$

Analyzing the tropical stratosphere in the Chapman+2 model, Match et al. (2024) demonstrated that the ozone layer can be approximated as being in an O-damped limit above 26 km (i.e., above the peak in $[O_3]$). The O-damped limit results from catalytic destruction of atomic oxygen, most importantly by the NO_x cycle. The atomic oxygen that is being catalytically damped in the O-damped limit must be liberated through photolysis of O_3, so the O-damped limit has a photolytic sink of O_3. The suppression of O_3 by photolysis of O_3 is evident by J_{O_3} appearing in the denominator of the O-damped limit (Eq. 18). In the photolytic sink regime, photochemical adjustment can be either stabilizing or destabilizing depending on whether J_{O_2} or J_{O_3} is more strongly affected by the overhead perturbation.

Below 26 km (i.e., below the peak in $[O_3]$), the stratospheric ozone layer can be approximated as being in an O_3-damped limit. The damping of O_3 arises primarily from transport, which dilutes ozone in the tropical lower stratosphere by upwelling ozone-poor air up from below. When the dominant sink of odd oxygen is from damping of O_3, the photolytic sink of O_3 no longer dictates the structure. This can be seen by the absence of J_{O_3} from Eq. 19. With this non-photolytic sink, only perturbations to J_{O_2} matter, and photochemical adjustment must be stabilizing. Thus, conventional explanations for self-healing and reverse self-healing are strictly true in the O_3-damped limit, and therefore capture the leading-order response to perturbations in the tropical lower stratosphere.

The O-damped limit and the Chapman Cycle both have a photolytic sink of O_3, and both produce ozone that scales as $(J_{O_2}/J_{O_3})^n$ (n = 1 for the O-damped limit and n=1/2 for the Chapman Cycle). Match et al. (2024). The photolytic sink of the O-damped limit arises because catalytic damping of atomic oxygen is rate-limited in atomic oxygen, whereas the photolytic sink of the Chapman Cycle arises because R4 is limited by the availability of atomic oxygen produced by photolysis of O_3. That the Chapman Cycle also has a photolytic sink means that it reproduces key photochemical sensitivities from the more-realistic

O-damped limit. This helps explain why Hartmann (1978), who analyzed a version of the Chapman Cycle that did not include explicit catalytic sinks or transport, nonetheless found photochemical destabilization at the correct altitude above 40 km in their tropical profile.

It has been suggested that self-healing and reverse self-healing are damped by transport, i.e., that photochemistry would stabilize a larger fraction of the UV anomaly if not for the damping effects of transport (Solomon et al., 1985). The fraction of photochemical stabilization is important because, in a hypothetical world with perfect photochemical stabilization, ozone-depleting substances that destroy ozone aloft would add exactly the same amount of ozone back through self-healing, eliminating anthropogenic impacts on the ozone layer. Thus, it is only the observed deviations below perfect stabilization that cause risks from ozone-depleting substances and benefits from their mitigation.

Does transport suppress the fraction of photochemical stabilization, as has been argued, by damping O_3 anomalies in the lower stratosphere? The answer is not clear-cut when the basic-state effects of the transport are accounted for, because although O_3 damping by transport certainly damps O_3, it also creates the O_3-damped regime of the lower stratosphere that is prone to photochemical stabilization. Transport introduces the possibility that O_3 depletion aloft can allow more ultraviolet fluxes below that speed up photochemical equilibration in the lower stratosphere, shifting down the transition altitude between the O_3-damped limit and the O-damped limit. Reflecting this nuance, increasing κ_{O_3} in the Chapman+2 model actually increases the fractional stabilization of the UV-locked O_3 anomaly from stratospheric cooling, while reducing the fractional stabilization of the UV-locked O_3 anomaly from O_3 depletion. Further work could clarify whether transport amplifies or suppresses this fraction of photochemical stabilization.

7.2 Photochemical destabilization is not an instability

Photochemical adjustment does not involve feedback, i.e., perturbations in ~~column ozone affect ozone~~ overhead column O_3 affect O_3 below a given altitude, but they do not affect ~~ozone~~ O_3 at that altitude. The effects of photochemical adjustment cascade downwards through the column. Absent a local feedback, photochemical destabilization cannot lead to a local photochemical instability in which ozone anomalies run away to become arbitrarily large or small. Photochemical adjustment can be analogized to a snowball rolling down a hill, which grows in proportion to itself in regions of destabilization and shrinks in proportion to itself in regions of stabilization. This analogy provides intuition to two key aspects of photochemical adjustment: (1) there is no local feedback (the snowball cannot grow while remaining stationary), and (2) the peak photochemical anomalies are set by the magnitude of destabilization and the depth of the atmosphere (length of the hill).

7.3 ~~The role of transport~~

~~The Chapman Cycle was successful at reproducing the photochemical regimes of MOBIDIC, in particular the transition from destabilization above 40 km to stabilization below 40 km in the tropics. However, below about 25 km in the tropics, transport of ozone is known to become a leading-order contributor to the ozone budget, and thus the Chapman Cycle assumption of photochemical equilibrium breaks down. Self-healing and reverse self-healing tend to occur lower in the stratosphere, often in this transport-dominated region. It has been argued that self-healing and reverse self-healing are damped by transport in~~

these regions (Solomon et al., 1985). The damping effects of transport on self-healing are important because, by opposing photochemical stabilization, transport can increase ultraviolet flux perturbations at the surface.

However, it appears that the overall effects of transport on self-healing and reverse self-healing might be nontrivial and potentially ambiguous. This is because transport opens up a non-equilibrium mechanism for photochemical stabilization: ozone depletion aloft can allow more ultraviolet fluxes below, speeding up photochemical equilibration in the lower stratosphere and shifting down the transition altitude between the transport-dominated regime and the photochemical-dominated regime. This transport-mediated mechanism occurs out of photochemical equilibrium and operates in addition to the photochemical equilibrium mechanisms considered in this paper. This transport pathway would seem to exclusively lead to photochemical stabilization, because ozone equilibrates more rapidly under stronger ultraviolet flux. The linear ozone model neglects this dependence of the ozone equilibration rate (A_2) on column ozone. Thus, compared to a motionless atmosphere, an atmosphere with transport might have an additional mechanism for self-healing and reverse self-healing through changes in the transition altitude between the transport-dominated regime and the photochemically-dominated regime. Because the effects of transport seem ambiguous, further work is needed to clarify whether it damps or amplifies self-healing and reverse self-healing.

7.3 Implications

Comprehensive photochemical models naturally produce realistic self-healing and reverse self-healing. Thus, the key advances of this paper are conceptual. They help analysts understand what mechanisms lead to robust model output. The interpretive advances of this work are most obvious when considering that a linear ozone model already contained regions of photochemical destabilization in the upper stratosphere that had not been described. The concept of photochemical The concepts of photochemical stabilization and destabilization accommodates explain major features of chemistry-climate model simulations that might have coexisted uneasily with previous theory. Nonetheless, this work also has methodological and physical implications that extend beyond understanding pre-existing model functionsphenomena.

A methodological implication of this work can be found in the construction of linear ozone models. In McCormack et al. (2006), a linear ozone model is formulated based on the model CHEM2D. In calculating the coefficients for the sensitivity to overhead column ozone perturbations, they encoded into their method the assumption that photolysis of ozone does not contribute to the destruction of ozone. Thus, they calibrated their sensitivities to perturbations in overhead column ozone based only on the effects of changes in the photolytic source of ozone. This approach appears to forbid photochemical destabilization by construction. Their approach is equivalent to our Lock Sink calculation in Figure Fig. 6, which was shown to induce large biases compared to a Fully Interactive calculationin the Chapman Cycle. It is possible that these biases could be smaller for a comprehensive calculation, but they do not appear to be *a priori* negligible. The evidence of strong photochemical destabilization in the Cariolle v2.9 model (Figure 3a) and the apparent success of the Chapman Cycle at reproducing that structure (Figure 3b) suggests that the Chapman sink cannot be discounted *a priori* when considering the photochemical sensitivity of the ozone layer. , especially in response to ozone depletion.

A physical implication of this work is that, because photochemical destabilization occurs below a threshold of overhead column ozone of roughly 10^{18} molec cm^{-2}, atmospheres with less ozone could have deeper regions of photochemical desta-

bilization. In today's tropical atmosphere, destabilization occurs above 40 km, encompassing approximately 4% of the ozone layer. This overhead column ozone threshold would occur at a much lower altitude and could encompass a much larger fraction of the ozone layer in an atmosphere with less total ozone. The atmosphere had lower ozone throughout much of Earth's history, over which atmospheric O_2 has increased by seven orders of magnitude, and overhead column ozone has correspondingly increased from being vanishingly small to its present values (Kasting and Donahue, 1980). If ozone increased continuously, then there must have been an era when total column ozone was approximately 10^{18} molec cm^{-2}, during which our theory predicts that the ozone layer ~~would have been maximally photochemically destabilizingall the way to the surface~~could have been completely photochemically destabilizing. This could have amplified the effects of processes that add or deplete ozone, thereby amplifying the variability of UV light reaching the surface, affecting early life. Similarly, planets outside our solar system could host ozone layers that are photochemically destabilizing. Ozone layers at varying concentrations of O_2 have been simulated using one-dimensional models (Kasting and Donahue, 1980; Levine, 1977; Segura et al., 2003) and recently chemistry-climate models (Cooke et al., 2022; Józefiak et al., 2023), but the photochemical sensitivity of the ozone layer has not been quantified for atmospheres with different amounts of O_2, a subject for future work.

8 Conclusions

~~The~~ It has long been known that the photochemical nature of the ozone layer ~~has long been known to cause~~ causes it to respond ~~in surprising ways~~ counterintuitively to perturbations. Ozone-depleting substances can lead to increases in ozone at some altitudes, known as self-healing, which have been argued to result from the increased ultraviolet fluxes reaching lower altitudes. Processes that increase ozone, such as stratospheric cooling, can lead to decreases in ozone below, known as reverse self-healing, which have been argued to result from the decreased ultraviolet fluxes reaching lower altitudes. We have pursued a quantitative characterization and understanding of the photochemical processes that lead to self-healing and reverse self-healing. To do so, we have defined photochemical adjustment as the component of the ozone response to a perturbation that results from changes in photolysis due to changes in ~~column ozone aloft~~overhead column ozone. Photochemical adjustment ~~can be~~ is quantified as the difference in the ozone response to a perturbation in a fully interactive photochemical experiment versus ~~in a photochemical experiment with ultraviolet~~ with UV fluxes locked to their ~~control profile~~unperturbed values.

Photochemical ~~adjustment was quantified using a linear emulator of the chemistry-climate model MOBIDIC based on the coefficients of the~~ sensitivities were quantified in two linear ozone models: Cariolle v2.9 and LINOZ. Photochemical adjustment was further quantified in column calculations using Cariolle v2.9 ~~linear ozone model. We studied~~ of the response to ozone depletion and stratospheric cooling. Photochemical adjustment can be stabilizing, damping overhead column ozone perturbations towards the surface, and potentially leading to self-healing and reverse self-healing. Self-healing and reverse self-healing only occur for the subset of photochemical stabilization in which the photochemical adjustment dominates the local effects of the perturbation~~. Thus, self-healing and reverse self-healing are often~~ , making them just the tip of the iceberg ~~of large~~ for often-large photochemical adjustment. We have also characterized a ~~significant~~ new and unconventional region of photochemical destabilization ~~,~~ above 40 km. ~~Photochemical destabilization is unconventional, given that photochemical~~

~~adjustment was previously only considered in the context of photochemical stabilization leading to self-healing and reverse self-healing.~~

The regimes of photochemical stabilization and destabilization in ~~MOBIDIC~~ the linear ozone models (Cariolle v2.9 and LINOZ) were successfully emulated using ~~the fundamental ChapmanCycle~~ a Chapman+2 model of the ozone layer~~. The Chapman Cycle~~, which augments the Chapman Cycle with generalized destruction of O and O_3 by catalytic cycles and transport. A column-by-column calculation using the Chapman+2 model reproduces the full latitudinal structure of the transition from destabilization to stabilization (~~Figure~~ Fig. 3). Photochemical destabilization in the Chapman~~Cycle~~ +2 model arises when the photolytic sink of ozone (absorption by O_3) is more sensitive than the photolytic source (absorption by O_2) to perturbations in overhead O_3. The sensitivity of the photolytic source and sink can in turn be related directly to the absorption spectra of O_2 and O_3. Photochemical destabilization occurs when absorption in the extension window ($\lambda > 240$ nm) ~~is becoming~~ becomes optically saturated ($\tau_{O_3} = 1$) while absorption in the overlap window ($\lambda < 240$ nm) remains unsaturated. Photochemical stabilization occurs once absorption by O_3 in the overlap window saturates. This spectral intuition leads to a simple theory that photochemical destabilization should occur below a threshold of slant overhead column ozone of approximately 10^{18} molec cm^{-2}, which reproduces the latitudinal structure of the transition altitude between destabilization and stabilization in ~~MOBIDIC~~ the linear ozone models and the Chapman~~Cycle~~+2 model.

Roughly 4% of ozone molecules in the tropics today are in a photochemically destabilizing regime. As considered in the Discussion as a subject for future work, an atmosphere with less total ozone will have a higher fraction of its ozone layer in a destabilizing regime below the overhead column ozone threshold of 10^{18} molec cm^{-2}. Over Earth's history, atmospheric O_2 has increased by at least seven orders of magnitude, leading to the formation of the ozone layer (e.g., Kasting and Donahue, 1980). Paleoclimatic ozone layers with total column ozone below the destabilization threshold could have been ~~destabilizing all the way down to the surface~~completely destabilizing, amplifying ozone perturbations and increasing the variability of UV light experienced by early life.

Code and data availability. The Chapman Cycle Photochemical Equilibrium Solver described in Section 4 is published at doi:10.5281/zenodo.10515738. CMIP6 data is accessible from https://esgf-node.llnl.gov/search/cmip6/.

Author contributions. Authors' contributions: AM and EPG acquired funding; AM, EPG, and SF conceptualized research; AM performed formal analysis; AM wrote original draft; EPG and SF reviewed and edited paper.

Competing interests. The authors declare that they have no conflict of interest.

Acknowledgements. ~~The authors~~ We thank Daniel Cariolle and Clara Orbe for sharing the latest ~~version (v2.9) of his~~ versions of their linear ozone model coefficients. A.M. acknowledges constructive discussions with Benjamin Schaffer, Nadir Jeevanjee, ~~and~~ Alison Ming, and Peter Hitchcock, and at the Princeton Center for Theoretical Science workshop *From Spectroscopy to Climate*. This work was supported by the National Science Foundation under Award No. 2120717 and OAC-2004572, and by Schmidt ~~Futures~~Sciences, a philanthropic initiative founded by Eric and Wendy Schmidt, as part of the Virtual Earth System Research Institute (VESRI). For the CMIP6 model output, we acknowledge the World Climate Research Programme, the climate modeling groups, and the Earth System Grid Federation (ESGF), as supported by multiple funding agencies.

References

Ackerman, M.: Ultraviolet Solar Radiation Related to Mesospheric Processes, pp. 149–159, Springer, Dordrecht, https://doi.org/10.1007/978-94-010-3114-1_11, 1971.

Andrews, D. G., Holton, J. R., and Leovy, C. B.: Middle Atmosphere Dynamics, Academic Press, 1987.

Bates, D. R. and Nicolet, M.: The Photochemistry of Atmospheric Water Vapor, Journal of Geophysical Research (1896-1977), 55, 301–327, https://doi.org/10.1029/JZ055i003p00301, 1950.

Brasseur, G. P. and Solomon, S.: Aeronomy of the Middle Atmosphere: Chemistry and Physics of the Stratosphere and Mesosphere, Springer, Dordrecht, Netherlands, 2005.

Cariolle, D. and Brard, D.: The Distribution of Ozone and Active Stratospheric Species: Results of a Two-Dimensional Atmospheric Model, in: Atmospheric Ozone, pp. 77–81, Greece, https://doi.org/10.1007/978-94-009-5313-0_16, 1984.

Cariolle, D. and Déqué, M.: Southern Hemisphere Medium-Scale Waves and Total Ozone Disturbances in a Spectral General Circulation Model, Journal of Geophysical Research: Atmospheres, 91, 10 825–10 846, https://doi.org/10.1029/JD091ID10P10825, 1986.

Cariolle, D. and Teyssèdre, H.: A Revised Linear Ozone Photochemistry Parameterization for Use in Transport and General Circulation Models: Multi-annual Simulations, Atmospheric Chemistry and Physics, 7, 2183–2196, https://doi.org/10.5194/ACP-7-2183-2007, 2007.

Chapman, S.: A Theory of Upper Atmospheric Ozone, Memoirs of the Royal Meteorological Society, III, 103–125, 1930.

Coddington, O., Lean, J., Lindholm, D., Pilewskie, P., and Snow, M.: NOAA Climate Data Record (CDR) of Solar Spectral Irradiance (SSI), Version 2.1, https://doi.org/10.7289/V53776SW, 2015.

Cooke, G. J., Marsh, D. R., Walsh, C., Black, B., and Lamarque, J.-F.: A Revised Lower Estimate of Ozone Columns during Earth's Oxygenated History, Royal Society Open Science, 9, 2022.

Craig, R. A.: The Upper Atmosphere: Meteorology and Physics, Academic Press, 1965.

Crutzen, P. J.: The Influence of Nitrogen Oxides on the Atmospheric Ozone Content, Quarterly Journal of the Royal Meteorological Society, 96, 320–325, https://doi.org/10.1002/qj.49709640815, 1970.

Crutzen, P. J.: Estimates of Possible Future Ozone Reductions from Continued Use of Fluoro-Chloro-Methanes (CF2Cl2, CFCl3), Geophysical Research Letters, 1, 205–208, https://doi.org/10.1029/GL001I005P00205, 1974.

DallaSanta, K., Orbe, C., Rind, D., Nazarenko, L., and Jonas, J.: Dynamical and Trace Gas Responses of the Quasi-Biennial Oscillation to Increased CO2, Journal of Geophysical Research: Atmospheres, 126, e2020JD034 151, https://doi.org/10.1029/2020JD034151, 2021.

Demore, W. B., Howard, C. J., Sander, S. P., Ravishankara, A. R., Golden, D. M., Kolb, C. E., Hampson, R. F., Molina, M. J., and Kurylo, M. J.: Chemical Kinetics and Photochemical Data for Use in Stratospheric Modeling Evaluation Number 12 NASA Panel for Data Evaluation, Tech. rep., Jet Propulsion Laboratory, Pasadena, CA, 1997.

Déqué, M., Dreveton, C., Braun, A., and Cariolle, D.: The ARPEGE/IFS Atmosphere Model: A Contribution to the French Community Climate Modelling, Climate Dynamics, 10, 249–266, https://doi.org/10.1007/BF00208992, 1994.

Dütsch, H. U.: The Search for Solar Cycle-Ozone Relationships, Journal of Atmospheric and Terrestrial Physics, 41, 771–785, https://doi.org/10.1016/0021-9169(79)90124-7, 1979.

Finlayson-Pitts, B. J. and Pitts, Jr., J. N.: Chemistry of the Upper and Lower Atmosphere: Theory, Experiments, and Applications, Academic Press, San Diego, CA, 2000.

Fomichev, V. I., Jonsson, A. I., de Grandpré, J., Beagley, S. R., McLandress, C., Semeniuk, K., and Shepherd, T. G.: Response of the Middle Atmosphere to CO2 Doubling: Results from the Canadian Middle Atmosphere Model, Journal of Climate, 20, 1121–1144, https://doi.org/10.1175/JCLI4030.1, 2007.

Galewsky, J., Sobel, A., Held, I., Galewsky, J., Sobel, A., and Held, I.: Diagnosis of Subtropical Humidity Dynamics Using Tracers of Last Saturation, Journal of the Atmospheric Sciences, 62, 3353–3367, https://doi.org/10.1175/JAS3533.1, 2005.

Groves, K. S., Mattingly, S. R., and Tuck, A. F.: Increased Atmospheric Carbon Dioxide and Stratospheric Ozone, Nature 1978 273:5665, 273, 711–715, https://doi.org/10.1038/273711a0, 1978.

Haigh, J. D. and Pyle, J. A.: Ozone Perturbation Experiments in a Two-Dimensional Circulation Model, Quarterly Journal of the Royal Meteorological Society, 108, 551–574, https://doi.org/10.1002/QJ.49710845705, 1982.

Hall, T. M. and Prather, M. J.: Seasonal Evolutions of N2O, O3, and CO2: Three-dimensional Simulations of Stratospheric Correlations, Journal of Geophysical Research: Atmospheres, 100, 16 699–16 720, https://doi.org/10.1029/94JD03300, 1995.

Hartmann, D. L.: A Note Concerning the Effect of Varying Extinction on Radiative-Photochemical Relaxation, Journal of the Atmospheric Sciences, 35, 1125–1130, 1978.

Hersbach, H., Bell, B., Berrisford, P., Hirahara, S., Horányi, A., Muñoz-Sabater, J., Nicolas, J., Peubey, C., Radu, R., Schepers, D., Simmons, A., Soci, C., Abdalla, S., Abellan, X., Balsamo, G., Bechtold, P., Biavati, G., Bidlot, J., Bonavita, M., De Chiara, G., Dahlgren, P., Dee, D., Diamantakis, M., Dragani, R., Flemming, J., Forbes, R., Fuentes, M., Geer, A., Haimberger, L., Healy, S., Hogan, R. J., Hólm, E., Janisková, M., Keeley, S., Laloyaux, P., Lopez, P., Lupu, C., Radnoti, G., de Rosnay, P., Rozum, I., Vamborg, F., Villaume, S., and Thépaut, J.-N.: The ERA5 Global Reanalysis, Quarterly Journal of the Royal Meteorological Society, 146, 1999–2049, https://doi.org/10.1002/qj.3803, 2020.

Hudson, R. D.: Chlorofluoromethanes and the Stratosphere, Tech. rep., NASA, Greenbelt, MD, 1977.

Jacob, D.: Introduction to Atmospheric Chemistry, Princeton University Press, 1999.

Johnston, H.: The Concorde, Oxides of Nitrogen, and Stratospheric Ozone, Search, 3, 276–282, 1972.

Jonsson, A. I., de Grandpré, J., Fomichev, V. I., McConnell, J. C., and Beagley, S. R.: Doubled CO2 -Induced Cooling in the Middle Atmosphere: Photochemical Analysis of the Ozone Radiative Feedback, Journal of Geophysical Research, 109, D24 103, https://doi.org/10.1029/2004JD005093, 2004.

Józefiak, I., Sukhodolov, T., Egorova, T., Chiodo, G., Peter, T., Rieder, H., Sedlacek, J., Stenke, A., and Rozanov, E.: Stratospheric Dynamics Modulates Ozone Layer Response to Molecular Oxygen Variations, Frontiers in Earth Science, 11, 2023.

Kasting, J. F. and Donahue, T. M.: The Evolution of Atmospheric Ozone, Journal of Geophysical Research, 85, 3255, https://doi.org/10.1029/JC085iC06p03255, 1980.

Levine, J. S.: The Evolution of Stratospheric Ozone, Ph.D. thesis, University of Michigan, 1977.

Match, A. and Gerber, E. P.: Tropospheric Expansion Under Global Warming Reduces Tropical Lower Stratospheric Ozone, Geophysical Research Letters, 49, e2022GL099 463, https://doi.org/10.1029/2022GL099463, 2022.

Match, A., Gerber, E. P., and Fueglistaler, S.: Protection without Poison: Why Tropical Ozone Maximizes in the Interior of the Atmosphere, EGUsphere, pp. 1–29, https://doi.org/10.5194/egusphere-2024-1552, 2024.

McCormack, J. P., Eckermann, S. D., Siskind, D. E., and McGee, T. J.: CHEM2D-OPP: A New Linearized Gas-Phase Ozone Photochemistry Parameterization for High-Altitude NWP and Climate Models, Atmospheric Chemistry and Physics, 6, 4943–4972, https://doi.org/10.5194/ACP-6-4943-2006, 2006.

McLinden, C. A., Olsen, S. C., Hannegan, B., Wild, O., Prather, M. J., and Sundet, J.: Stratospheric Ozone in 3-D Models: A Simple Chemistry and the Cross-Tropopause Flux, Journal of Geophysical Research: Atmospheres, 105, 14 653–14 665, https://doi.org/10.1029/2000JD900124, 2000.

Meraner, K., Rast, S., and Schmidt, H.: How Useful Is a Linear Ozone Parameterization for Global Climate Modeling?, Journal of Advances in Modeling Earth Systems, 12, e2019MS002 003, https://doi.org/10.1029/2019MS002003, 2020.

Meul, S., Langematz, U., Oberländer, S., Garny, H., and Jöckel, P.: Chemical Contribution to Future Tropical Ozone Change in the Lower Stratosphere, Atmos. Chem. Phys, 14, 2959–2971, https://doi.org/10.5194/acp-14-2959-2014, 2014.

NAS: Halocarbons: Effects on Stratospheric Ozone, Halocarbons, https://doi.org/10.17226/19978, 1976.

Pierrehumbert, R. T. and Roca, R.: Evidence for Control of Atlantic Subtropical Humidity by Large Scale Advection, Geophysical Research Letters, 25, 4537–4540, https://doi.org/10.1029/1998GL900203, 1998.

Ratner, M. I. and Walker, J. C. G.: Atmospheric Ozone and the History of Life, Journal of the Atmospheric Sciences, 29, 1972.

Rind, D., Jonas, J., Balachandran, N. K., Schmidt, G. A., and Lean, J.: The QBO in Two GISS Global Climate Models: 1. Generation of the QBO, Journal of Geophysical Research: Atmospheres, 119, 8798–8824, https://doi.org/10.1002/2014JD021678, 2014.

Sander, S. P., Abbatt, J., Barker, J. R., Burkholder, J. B., Friedl, R. R., Golden, D. M., Huie, R. E., Kolb, C. E., Kurylo, M. J., Moortgat, G. K., Orkin, V. L., and Wine, P. H.: Chemical Kinetics and Photochemical Data for Use in Atmospheric Studies, Evaluation No. 17, Tech. Rep. 10-6, Jet Propulsion Laboratory, Pasadena, CA, 2010.

Segura, A., Krelove, K., Kasting, J. F., Sommerlatt, D., Meadows, V., Crisp, D., Cohen, M., and Mlawer, E.: Ozone Concentrations and Ultraviolet Fluxes on Earth-Like Planets Around Other Stars, Astrobiology, 3, 2003.

Sherwood, S. C.: Maintenance of the Free-Tropospheric Tropical Water Vapor Distribution. Part II: Simulation by Large-Scale Advection, Journal of Climate, 9, 1996.

Solomon, S., Garcia, R. R., and Stordal, F.: Transport Processes and Ozone Perturbations, Journal of Geophysical Research: Atmospheres, 90, 12 981–12 989, https://doi.org/10.1029/JD090ID07P12981, 1985.

WMO: Atmospheric Ozone: Assessment of Our Understanding of the Processes Controlling Its Present Distribution and Change, Tech. rep., 1985.

WMO: Scientific Assessment of Ozone Depletion: 2018, Tech. rep., WMO (World Meteorological Organization), Geneva, Switzerland, 2018.

Wuebbles, D. J., Luther, F. M., and Penner, J. E.: Effect of Coupled Anthropogenic Perturbations on Stratospheric Ozone, Journal of Geophysical Research: Oceans, 88, 1444–1456, https://doi.org/10.1029/JC088IC02P01444, 1983.